Phase-field simulation of recrystallization and grain growth : description of MICRESS software and application in Al-Mg-Sc-Zr alloy

BY

Georgakou Artemis-Georgia

A Thesis submitted in partial fulfillment of the requirements for the degree of

Diploma in Mechanical Engineering

at the

UNIVERCITY OF THESSALY

DEPARTMENT OF MECHANICAL ENGINEERING

Thesis Advisor: Prof. G.N.Haidemenopoulos

June 2013

ABSTRACT

The objective of this thesis was the simulation of the recrystallization and grain growth of a single-phase Aluminium–Magnesium (5xxx) alloy containing Scandium and Zirconium additions. The alloy has already been cold worked and undergone annealing. During annealing, recrystallization and grain growth occurred. Three initial conditions have been considered. The first one regards to the influence of the stored energy on the recrystallized volume fraction. The second one regards to the influence of the initial average grain size of the microstructure on the recrystallized volume fraction. The third one regards to the contribution of pinning force of $Al_3(Sc,Zr)$ particles on the average grain radius of the final microstructure.

Recrystallization and grain growth simulations of the Al-Mg-Sc-Zr alloy have been carried out using MICRESS software, which is based on the phase-field method. Numerical data from relevant published literature, such as the stored energy and the pinning force, were used as input data in the simulations.

The phase field method is developing as a versatile tool for simulating microstructure evolution phenomena. The main objective of this thesis has been to study the effects of finely dispersed $Al_3(Sc,Zr)$ precipitates on recrystallization and grain growth using computer simulations based on a diffuse-interface 2D phase-field kinetic model. The results of these simulations contribute in the prediction of the recrystallized volume fraction and the average grain size at a specific temperature and time space. The results show that the finely dispersed $Al_3(Sc,Zr)$ particles exert a strong pinning effect on the grain boundaries. Implications of these results for grain size control in Al-Mg based alloys are discussed.

ACKNOWLEDGEMENTS

I would like to express my appreciation to my advisor: Dr. G.N.Haidemenopoulos. Thanks for giving me the opportunity to be part of the Materials Laboratory. Special thanks for his time, patience, and understanding. It has been an honor to work with you. My gratitude also goes to the Material Laboratory; there are not enough words to describe your excellent work.

TABLE OF CONTENTS

LIST OF FIGURES

LIST OF TABLES

1. INTRODUCTION

The macroscopic behavior of metallic materials is to a large extent controlled by the size and shape of the grains that constitute the material microstructure. The microlevel grain structure will influence macroscopic material properties such as mechanical strength, electrical conductivity, wear and corrosion resistance, ductility, hardness and fatigue resistance. Being able to predict and control the morphology of this microstructure during different metal working processes thus allows the development of tailored material properties, optimized products and more efficient production processes. Understanding and manipulating the material microstructure are key components in the production of functionally graded materials, having engineered properties in different regions. Fine-grained materials, with grain sizes down to the nanoscale, are becoming increasingly important in many applications, e.g., in the miniaturization of products such as micro-electro-mechanical components (MEMS), in biomedical devices and also in the production of thin metallic films and foils. As one or more physical dimensions of the product are reduced, the microstructure has to be tailored correspondingly in order to maintain required material properties and reliable operation of the product. Recrystallization and grain size control is also of primary interest in the development of high strength steels. From these observations it is clear that grain size and recrystallization are fundamental concepts in materials science and in materials design.

Traditional aluminium alloys for high performance applications, such as Al 7075, have maximum use temperatures in the 150–170 °C range. Above this, alloy strength degrades quickly with time in service due to rapid coarsening of fine strengthening precipitates. Applications that have a maximum use temperature above this range are required to use a material with a much higher density, such as titanium or steel. The capability of utilizing an aluminium alloy in such applications would result in significant weight savings and likely a reduction in both cost and lead time for component production.

Significant past research has been conducted to develop new Al alloys with good high temperature properties. Many of the approaches included non-age-hardenable systems with thermodynamically stable precipitates for high temperature strength. Significant improvements were shown for systems such as Al-Fe-Ce and Al-Fe-V-Si, where the principle strengthening phases are incoherent intermetallic particles. An alternate approach is to use coherent intermetallic precipitates for strengthening. Only a limited number of possibilities exist in Al-based alloys for the formation of coherent strengthening particles that are thermodynamically stable and have the ordered, L_{12} structure [1]. Of the possibilities, additions of Er and Sc have been most commonly studied [1] and [2]. Er additions form the L_{12} ordered Al_3Er phase. While Er is less expensive than Sc and has a smaller freezing range, the lattice constant, approximately 0.422 nm [1], is significantly larger than that of Al, so that it is difficult to retain particle coherency to a useful size. Further, the density of Er-containing alloys is significantly higher than comparable alloys based on Sc.

A significant amount of research has been carried out on Sc-containing Al alloys over the last 20 years, owing to the improved properties that can be obtained by a Sc addition [3-10]. One of the most important advantages is related to the formation of a dense and homogeneous distribution of precipitates during thermomechanical processing at elevated temperatures, which in turn leads to an efficient control of the microstructure of the alloy [11,12]. Aluminium forms a thermodynamically stable Al_3Sc phase with scandium additions. Sc has a very low solid solubility in Al, approximately 0.4 wt% at the eutectic temperature. For this reason, solutionizing near the eutectic temperature

followed by quenching to re-precipitate fine, dispersed Al_3Sc particles would be largely ineffective. The lattice parameter of the Al_3Sc phase, 0.410 nm, matches very closely to that of the aluminium matrix, 0.405 nm. Al_3Sc has the L_{12} type ordered face-centered cubic structure and should form coherent precipitates below a size of approximately 50 nm. The similarity of the lattice parameter and structure of Al_3Sc to those of the aluminium matrix is expected to reduce the driving force for coarsening of the Al_3Sc particles. Fine Al_3Sc precipitates that are coherent with the matrix are expected to contribute to the alloy strength through dislocation-particle interactions, as is the case in nickel-based superalloys.

Addition of magnesium provides both solid solution strengthening and increases the lattice parameter of the aluminium matrix, which provides a better match with Al_3Sc and further decreases the driving force for coarsening of the Al_3Sc particles. The magnesium in the commercial alloys ranges all the way from 0.5 to 12-13% Mg, the low-magnesium alloys having the best formability, the high-magnesium reasonably good castability and high strength. It is normal practice to prepare these alloys from the higher grades of aluminium (99.7 or better) to obtain maximum corrosion resistance and reflectivity; thus the iron and silicon contents are usually lower than in other aluminium alloys. Iron and zirconium are sometimes added to increase the recrystallization temperature.

It is well known that adding Sc in combination with Zr leads to a higher temperature stability of the precipitates (slower rate of coarsening) as compared with a Sc addition alone. The Al_3Sc phase can dissolve a considerable amount of Zr when Sc and Zr are added in combination. The precipitates are frequently denoted as $Al_3(Sc_{1-x}Zr_x)$. It has been discovered that, due to the faster diffusion rate of Sc as compared with Zr, the formation of these precipitates starts with almost pure Al_3Sc whereas the Zr content gradually increases during growth of the precipitates, leading to a core/shell structure of the precipitates. The high price of Sc is prohibitive for extended commercial applications of Sc-containing aluminium alloys. At present, the use is limited to high-end sporting equipment and to a few aerospace applications. In order to draw the benefit of Sc addition in other product ranges, it is necessary to minimize the associated cost by establishing the minimum Sc content necessary for obtaining the desired effect. It has been found that zirconium substitutes for Sc in Al_3Sc in up to 1/3 of the Sc lattice sites. It is believed that as a slow diffuser in aluminium, the zirconium will additionally stabilize these $Al_3(Sc,Zr)$ precipitates.

The addition of Sc to Al-based alloys is a very effective means of increasing their resistance to recrystallization [13] and [14] via the formation of a high density of Al_3Sc precipitates that pin grain and subgrain boundaries. These precipitates also cause hardening. In fact, Sc produces the largest increase in hardness per atomic percent of solute. Addition of Zr together with Sc improves the effectiveness of Sc as an inhibitor of recrystallization and increases the stability of the alloy during prolonged annealing at high temperatures [13]. The addition of Zr reduces the susceptibility of the Al_3Sc precipitates to coarsening. Analysis in bulk material has shown that Zr dissolves in the Al_3Sc phase by replacing Sc, thus forming $Al_3(Sc_{1-x}Zr_x)$. The maximum solubility given by Harada et al. corresponds to $x=0.5$ [15], although these authors also report the existence of a compound with $x=0.75$. It has therefore been assumed that the precipitates in Al–Sc–Zr alloys are composed of a stoichiometric $Al_3(Sc,Zr)$ phase with a random distribution of Sc and Zr on Sc sublattice sites. However, it is not obvious that the behavior of nm-size precipitates should follow that of the bulk. Whereas the effect of Sc and Zr on mechanical properties of Al alloys is already well documented,

relatively little research has been performed on the morphology and phase distribution of precipitates in the ternary alloys.

The drive to further understand recrystallization in aluminium alloys stems from the presence of hard second- phase particles in most commercially important alloys, and the dependence of strength and formability on the final grain size and shape. Large particles present in the microstructure, typically from casting, can act as efficient nuclei for recrystallization due to the large amount of stored energy that concentrated next to them during cold rolling. Additionally, small precipitates can act to inhibit recrystallization and pin grain boundaries through a Zener drag process. Forming operations such as superplasticity typically require either a fine, stable grain structure or a substructure that is stable against recrystallization even at temperatures near the melting point. There has been recent interest in using the low cost aluminium alloy 5083 for superplastic deformation This alloy contains from 4-5 wt.% Mg in solid solution with Mn and Cr added to form precipitates which stabilize the grain size and increase strength.

Previous studies on manipulating the precipitate structure through heat treatments and alloying additions have resulted in increased elongation and finer grains. Interestingly, though, the addition of Zr to 5083 resulted in an increased grain size . Recrystallization in these materials has been observed to nucleate primarily on the eutectic constituent particles (ECs) that form during casting, though some nucleation also occurs on large precipitates. Additions of Sc to Al-Mg alloys results in the formation of fine, coherent, spherical precipitates of Al_3Sc which suppresses recrystallization [15,16]. When alloyed with Zr, it has been observed that the Zr can replace Sc in the precipitate at up to 50 at.%, and results in a precipitate more stable against coarsening at high temperatures.

This paper reports on studies of recrystallization and grain growth in Al-Mg alloys containing Sc and Zr in an effort to understand the role of particle type and morphology on the recrystallization kinetics and the resultant grain structure. It is based on previous published work [17] on computational alloy thermodynamics. In [17] the grain refinement potential has been assessed by Scheil-Gulliver simulations of solidification paths, while the recrystallization resistance (Zener drag) has been assessed by calculation of the precipitation driving forces of the Al_3Sc and Al_3Zr intermetallics. The objective of the current work is to simulate the recrystallization and grain growth of an Al-M-g-Sc-Zr alloy. MICRESS (MICRostructure Evolution Simulation Software) is used in order to fulfill the simulations. Grain growth in single-phase materials has been simulated several times with the phase field method[16], [18], [19] and [20]. Two-dimensional phase field simulations of Zener pinning were discussed in [18], [20], [21],[22] and [23]. Numerical data from equivalent papers was used to determine the detailed microstructural characterization needed for the simulations.

2. LITERATURE REVIEW

2.1 Recrystallization

Recrystallization is a process by which deformed grains are replaced by a new set of undeformed grains that nucleate and grow until the original grains have been entirely consumed. Recrystallization is usually accompanied by a reduction in the strength and hardness of a material and a simultaneous increase in the ductility. Thus, the process may be introduced as a deliberate step in metals processing or may be an undesirable byproduct of another processing step. The most important industrial uses are the softening of metals previously hardened by cold work, which have lost their ductility, and the control of the grain structure in the final product.

It can be defined as the temperature at which destroyed grains of a crystal structure are replaced by the new strain free grains.

A precise definition of recrystallization is difficult to state as the process is strongly related to several other processes, most notably recovery and grain growth. In some cases it is difficult to precisely define the point at which one process begins and another ends. Doherty et al. [24] defined recrystallization as:

"... the formation of a new grain structure in a deformed material by the formation and migration of high angle grain boundaries driven by the stored energy of deformation. High angle boundaries are those with greater than a 10-15° misorientation"

Thus the process can be differentiated from recovery (where high angle grain boundaries do not migrate) and grain growth (where the driving force is only due to the reduction in boundary area).

Recrystallization may occur during or after deformation (during cooling or a subsequent heat treatment, for example). The former is termed dynamic while the latter is termed static. Static recrystallization occurs on heating the deformed material to an elevated temperature. Dynamic recrystallization occurs during the plastic deformation. This only occurs for hot deformation at temperatures greater than 0.5 of the melting point. In addition, recrystallization may occur in a discontinuous manner, where distinct new grains form and grow, or a continuous manner, where the microstructure gradually evolves into a recrystallized microstructure. In most materials, temperatures $> T_m/3$ are required for recrystallization to proceed at a measurable rate, while grain boundaries are slowed down by the presence of solute and most practical materials have significant amounts of solute. The different mechanisms by which recrystallization and recovery occur are complex and in many cases remain controversial.

There are several, largely empirical laws of recrystallization:

- *Thermally activated*. The rate of the microscopic mechanisms controlling the nucleation and growth of recrystallized grains depend on the annealing temperature. Arrhenius-type equations indicate an exponential relationship.
- *Critical temperature*. Following from the previous rule it is found that recrystallization requires a minimum temperature for the necessary atomic mechanisms to occur. This recrystallization temperature decreases with annealing time.

- *Critical deformation*. The prior deformation applied to the material must be adequate to provide nuclei and sufficient stored energy to drive their growth.
- *Deformation affects the critical temperature*. Increasing the magnitude of prior deformation (Fig.1), or reducing the deformation temperature, will increase the stored energy and the number of potential nuclei. As a result the recrystallization temperature will decrease with increasing deformation.
- *Initial grain size affects the critical temperature*. Grain boundaries are good sites for nuclei to form. Since an increase in grain size results in fewer boundaries this results in a decrease in the nucleation rate and hence an increase in the recrystallization temperature.
- *Deformation affects the final grain size*. Increasing the deformation, or reducing the deformation temperature, increases the rate of nucleation faster than it increases the rate of growth. As a result the final grain size is reduced by increased deformation.

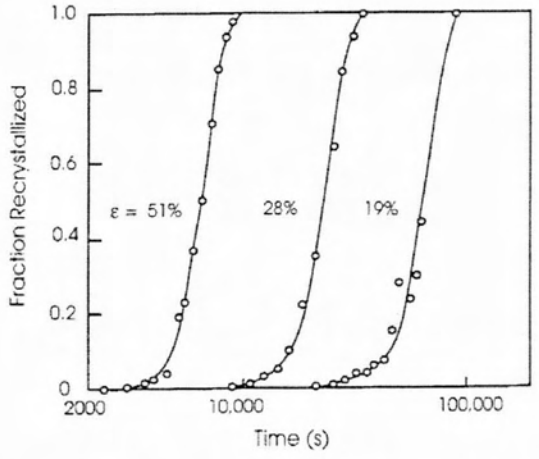

[Humphreys]

Figure 1: **The effect of tensile strain on the recrystallization kinetics of aluminium annealed at 350 ^{0}C, (Anderson and Mehl 1945).**

During plastic deformation the work performed is the integral of the stress and the plastic strain increment. Although the majority of this work is converted to heat, some fraction (~1-5%) is retained in the material as defects - particularly dislocations. The rearrangement or elimination of these dislocations will reduce the internal energy of the system and so there is a thermodynamic driving force for such processes. At moderate to high temperatures, particularly in materials with a high stacking fault energy such as aluminium and nickel, recovery occurs readily and free dislocations will readily rearrange themselves into subgrains surrounded by low-angle grain boundaries. The driving force is the difference in energy between the deformed and recrystallized state ΔE which can be determined by the dislocation density or the subgrain size and boundary energy):

$$\Delta E \approx \rho G b^2 \approx 3 \gamma_s / d_s \qquad (1)$$

where ρ is the dislocation density, G is the shear modulus, b is the Burgers vector of the dislocations, γ is the sub-grain boundary energy and d_s is the subgrain size.

Historically it was assumed that the nucleation rate of new recrystallized grains would be determined by the thermal fluctuation model successfully used for solidification and precipitation phenomena. In this theory it is assumed that as a result of the natural movement of atoms (which increases with

temperature) small nuclei would spontaneously arise in the matrix. The formation of these nuclei would be associated with an energy requirement due to the formation of a new interface and an energy liberation due to the formation of a new volume of lower energy material. If the nuclei were larger than some critical radius then it would be thermodynamically stable and could start to grow. The main problem with this theory is that the stored energy due to dislocations is very low (0.1-1 Jm^{-3}) while the energy of a grain boundary is quite high (~0.5Jm^{-2}). Calculations based on these values found that the observed nucleation rate was greater than the calculated one by some impossibly large factor (~10^{50}).

As a result the alternate theory proposed by Cahn [25] is now universally accepted. The recrystallized grains do not nucleate in the classical fashion but rather grow from pre-existing sub-grains and cells. The 'incubation time' is then a period of recovery where sub-grains with low-angle boundaries (<1-2°) begin to accumulate dislocations and become increasingly misoriented with respect to their neighbors. The increase in misorientation increases the mobility of the boundary and so the rate of growth of the sub-grain increases. If one sub-grain in a local area happens to have an advantage over its neighbors (such as locally high dislocation densities, a greater size or favorable orientation) then this sub-grain will be able to grow more rapidly than its competitors. As it grows its boundary becomes increasingly misoriented with respect to the surrounding material until it can be recognized as an entirely new strain-free grain.

Recrystallization kinetics are commonly observed to follow the profile shown in Fig 2. There is an initial 'nucleation period' t_0 where the nuclei form, and then begin to grow at a constant rate consuming the deformed matrix. Although the process does not strictly follow classical nucleation theory it is often found that such mathematical descriptions provide at least a close approximation. For an array of spherical grains the mean radius R at a time t is [26]:

$$R = G\,(t - t_0) \tag{2}$$

where t_0 is the nucleation time and G is the growth rate dR/dt. If N nuclei form in the time increment dt and the grains are assumed to be spherical then the volume fraction f will be:

$$f = \frac{4}{3}\pi \dot{N} G^3 \int_0^t (t - t_0)^3 dt = \frac{\pi}{3} N G^3 t^4 \tag{3}$$

This equation is valid in the early stages of recrystallization when $f<<1$ and the growing grains are not impinging on each other. Once the grains come into contact the rate of growth slows and is related to the fraction of untransformed material by the Johnson-Mehl equation:

$$f = 1 - \exp\left(-\frac{\pi}{3} N G^3 t^4\right) \tag{4}$$

While this equation provides a better description of the process it still assumes that the grains are spherical, the nucleation and growth rates are constant, the nuclei are randomly distributed and the nucleation time t_0 is small. In practice few of these are actually valid and alternate models need to be used.

It is generally acknowledged that any useful model must not only account for the initial condition of the material but also the constantly changing relationship between the growing grains, the deformed matrix and any second phases or other microstructural factors. The situation is further complicated in dynamic systems where deformation and recrystallization occur simultaneously. As a result it has generally proven impossible to produce an accurate predictive model for industrial processes without

resorting to extensive empirical testing. Since this may require the use of industrial equipment that has not actually been built there are clear difficulties with this approach.

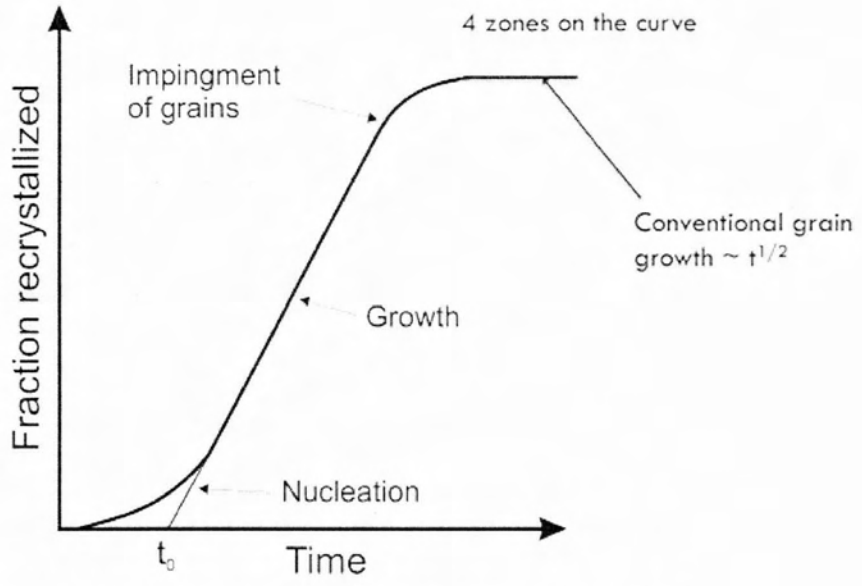

Figure 2: **Typical recrystallization kinetics during isothermal annealing.**

The traditional method to measure recrystallization is to perform optical metallography on sectioned samples. Recrystallized grains appear as approximately equiaxed grains with uniform color. Unrecrystallized grains appear as deformed grains with irregular contrast. Measurement is primarily the area fraction of recrystallized versus unrecrystallized material. Stereology tells us that this area fraction is equivalent to the volume fraction of recrystallized material. An easier measurement is hardness which decreases during the recrystallization process.

2.2 Grain Growth

Grain growth is the increase in size of grains (crystallites) in a material at high temperature. This occurs when recovery and recrystallisation are complete and further reduction in the internal energy can only be achieved by reducing the total area of grain boundary. The term is commonly used in metallurgy but is also used in reference to ceramics and minerals.

Importance of grain growth

Most materials exhibit the Hall–Petch effect at room-temperature and so display a higher yield stress when the grain size is reduced. At high temperatures the opposite is true since the open, disordered nature of grain boundaries means that vacancies can diffuse more rapidly down boundaries leading to more rapid Coble creep. Since boundaries are regions of high energy they make excellent sites for the nucleation of precipitates and other second-phases e.g. Mg–Si–Cu phases in some aluminium alloys or martensite platlets in steel. Depending on the second phase in question this may have positive or negative effects.

$$\sigma_y = \sigma i + \frac{k_y}{\sqrt{D}} \qquad (5)$$

where k_y is the Petch parameter, also known as unpinning constant.

Rules of Grain Growth

Grain growth has long been studied primarily by the examination of sectioned, polished and etched samples under the optical microscope. Although such methods enabled the collection of a great deal of empirical evidence, particular with regard to factors such as temperature or composition, the lack of crystallographic information limited the development of an understanding of the fundamental physics. Nevertheless, the following became well-established features of grain growth:

1. Grain growth occurs by the movement of grain boundaries and not by coalescence.
2. Boundary movement is discontinuous and the direction of motion may change suddenly.
3. One grain may grow into another grain whilst being consumed from the other side.
4. The rate of consumption often increases when the grain is nearly consumed.
5. A curved boundary typically migrates towards its centre of curvature.
6. When grain boundaries in a single phase meet at angles other than 120 degrees, the grain included by the more acute angle will be consumed so that the angles approach 120 degrees.

During the growth process, the grain structure undergoes topological changes. In two dimensions, von Neumann and Mullins[27] and [28] showed that the rate growth of n-sided grain is written as:

$$\frac{dA}{dt} = \frac{\pi}{3} \mathrm{m}\, \gamma\, (\mathrm{n} - 6) \tag{6}$$

where A is the grain area, m and γ are respectively the mobility and the specific energy of grain boundary. A grain with $n > 6$ will grow, whereas a grain with $n > 6$ will shrink.
Aboav [29] first noted a correlation between the number of sides of a grain, n, and the average number of sides, m_n, of its neighbors. It is found that m_n is linearly related to $1/n$. On the basis of Euler's theorem, Weaire [30] suggested a more general equation.

In the ideal case of isotropic boundary energies and mobolities, the first statistical grain growth model is proposed by Hillert [31] in 1965 with the mean growth velocity for grains of size R:

$$\frac{dR}{dt} = \alpha\, \mathrm{m}\, \gamma \left(\frac{1}{R_c} - \frac{1}{R}\right) \tag{7}$$

where α is a dimensionless constant ($\alpha = 0.5$ for 2-D) and R_c is a critical radius which being equal to the matrix mean grain radius R. A grain with $R > Rc$ will grow, whereas a grain with $R > Rc$ will shrink. In order to make his model congruent with the von Neumann n-6 law (Eq. (6)), Hillert proposed the following equation for n:

$$\mathrm{n} = 3\left(1 + \frac{R}{\bar{R}}\right) \tag{8}$$

where $\bar{R}$ is the average size of the neighbors.

Driving Force for Grain Growth

The boundary between one grain and its neighbour (grain boundary) is a defect in the crystal structure and so it is associated with a certain amount of energy. As a result, there is a thermodynamic driving force for the total area of boundary to be reduced. If the grain size increases, accompanied by a reduction in the actual number of grains per volume, then the total area of grain boundary will be reduced.

The local velocity of a grain boundary at any point is proportional to the local curvature of the grain boundary, i.e.:

$$\upsilon = M \gamma \kappa \tag{9}$$

where υ is the velocity of grain boundary, M is grain boundary mobility (generally depends on orientation of two grains), γ is the grain boundary energy and κ is the sum of the two principal surface curvatures.

Normal vs abnormal Grain Growth

In common with recovery and recrystallization, growth phenomena can be separated into continuous and discontinuous mechanisms (Fig. 3). In the former the microstructure evolves from state A to B (in this case the grains get larger) in a uniform manner. In the latter, the changes occur heterogeneously and specific transformed and untransformed regions may be identified. Discontinuous grain growth is characterised by a subset of grains growing at a high rate and at the expense of their neighbours and tends to result in a microstructure dominated by a few very large grains. In order for this to occur the subset of grains must possess some advantage over their competitors such as a high grain boundary energy, locally high grain boundary mobility, favourable texture or lower local second-phase particle density.

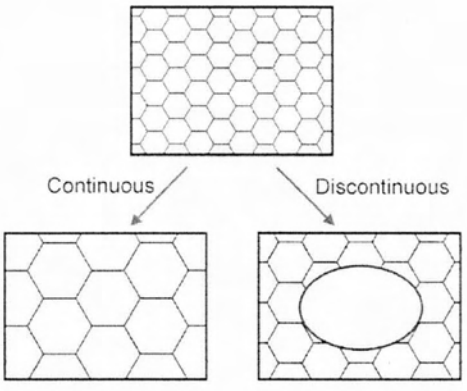

Figure 3: **The distinction between continuous (normal) grain growth, where all grains grow at roughly the same rate, and discontinuous (abnormal) grain growth, where one grain grows at a much greater rate than its neighbours.**

Factors influencing the rate of recrystallization

The annealing temperature has a dramatic influence on the rate of recrystallization which is reflected in the above equations. However, for a given temperature there are several additional factors that will influence the rate.

The rate of recrystallization is heavily influenced by the amount of deformation and, to a lesser extent, the manner in which it is applied. Heavily deformed materials will recrystallize more rapidly than those deformed to a lesser extent. Indeed, below a certain deformation recrystallization may never occur. Deformation at higher temperatures will allow concurrent recovery and so such materials will recrystallize more slowly than those deformed at room temperature e.g. contrast hot and cold rolling. In certain cases deformation may be unusually homogeneous or occur only on specific crystallographic planes. The absence of orientation gradients and other heterogeneities may prevent the formation of viable nuclei. Experiments in the 1970s found that molybdenum deformed to a true strain of 0.3, recrystallized most rapidly when tensioned and at decreasing rates for wire drawing, rolling and compression.

The orientation of a grain and how the orientation changes during deformation influence the accumulation of stored energy and hence the rate of recrystallization. The mobility of the grain boundaries is influenced by their orientation and so some crystallographic textures will result in faster growth than others.

Solute atoms, both deliberate additions and impurities, have a profound influence on the recrystallization kinetics. Even minor concentrations may have a substantial influence e.g. 0.004% Fe increases the recrystallization temperature by around 100°C (Humphreys and Hatherly [26]). It is currently unknown whether this effect is primarily due to the retardation of nucleation or the reduction in the mobility of grain boundaries i.e. growth.

Factors hindering Grain Growth

If there are additional factors preventing boundary movement, such as Zener pinning by particles, then the grain size may be restricted to a much lower value than might otherwise be expected. This is an important industrial mechanism in preventing the softening of materials at high temperature.

Influence of second phase particles on recrystallization

Many alloys of industrial significance have some volume fraction of second phase particles, either as a result of impurities or from deliberate alloying additions. Depending on their size and distribution such particles may act to either encourage or retard recrystallization.

2.3 Small particles – Pinning force

The presence of a particle distribution, in a polycrystalline structure, can influence the grain growth by pinning of their boundaries. The interaction of particles with grain boundaries is commonly known under Zener pinning [32]. For inhibiting curvature driven grain growth, Zener noted that the grain growth stops when the matrix mean grain size achieves the limiting value:

$$R_L = \frac{4r}{3f_v} \tag{10}$$

where r and f_v are respectively the average radius and the volume fraction of the particles.

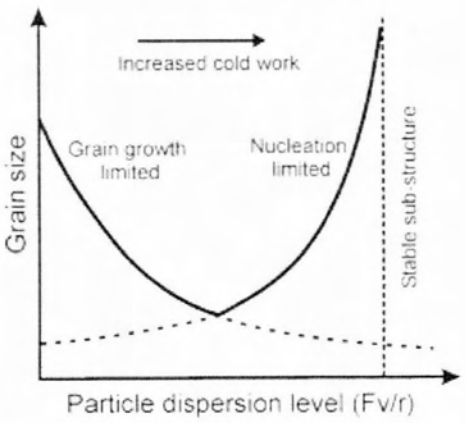

Figure 4: **The effect of a distribution of small particles on the grain size in a recrystallized sample. The minimum size occurs at the intersection of the growth stabilized.**

Recrystallization is prevented or significantly slowed by a dispersion of small, closely spaced particles due to Zener pinning on both low- and high-angle grain boundaries. This pressure directly opposes the driving force arising from the dislocation density and will influence both the nucleation and growth kinetics (Fig. 4). The effect can be rationalized with respect to the particle dispersion level f_v / r where f_v is the volume fraction of the second phase and r is the radius. At low f_v /r the grain size is determined by the number of nuclei, and so initially may be very small. However the grains are unstable with respect to grain growth and so will grow during annealing until the particles exert sufficient pinning pressure to halt them. At moderate f_v /r the grain size is still determined by the number of nuclei but now the grains are stable with respect to normal growth (while abnormal growth is still possible). At high f_v / r the unrecrystallized deformed structure is stable and recrystallization is suppressed.

The study of the collective influence of particles concerns a random particle distribution. In real materials, particles are not randomly distributed and can be of different pinning efficiency. The interaction of grain boundaries with particles occurs in a selective way. Currently, it is very difficult to include this preferential interaction directly in simulation models. The theory that predicts growth kinetics versus the temporal evolution of grain topology in the presence of particles is still lacking.

Origin of the Pinning force

A boundary is an imperfection in the crystal structure and as such is associated with a certain quantity of energy. When a boundary passes through an incoherent particle then the portion of boundary that would be inside the particle essentially ceases to exist. In order to move past the particle some new boundary must be created, and this is energetically unfavourable. While the region of boundary near the particle is pinned the rest of the boundary continues trying to move forward under its own driving force. This results in the boundary becoming bowed between those points where it is anchored to the particles.

Mathematical description of the Pinning force

Figure 5 illustrates a boundary of energy γ per unit area where it intersects with an incoherent particle of radius r. The pinning force acts along the line of contact between the boundary and the particle i.e. a circle of diameter AB = $2\pi r \cos\theta$ (Fig.6). The force per unit length of boundary in contact is $\gamma \sin\theta$. Hence the total force acting on the particle-boundary interface is:

$$F = 2 \pi r \gamma \cos\theta \sin\theta \quad (11)$$

The maximum restraining force occurs when $\theta = 45°$ and so $F_{max} = \pi r \gamma$.

In order to determine the pinning force by a given dispersion of particles, Clarence Zener made several important assumptions:

- The particles are spherical.
- The passage of the boundary does not alter the particle-boundary interaction.
- Each particle exerts the maximum pinning force on the boundary regardless of contact position.
- The contacts between particles and boundaries are completely random.
- The number density of particles on the boundary is that expected for a random distribution of particles.

For a volume fraction f_v of randomly distributed spherical particles of radius r, the number per unit volume (number density) is given by:

$$N_{total} = \frac{3 f_v}{4 \pi r^3} \quad (12)$$

From this total number density only those particles that are within one particle radius will be able to interact with the boundary. If the boundary is essentially planar then this fraction will be given by:

$$N_{interact} = 2r\, N_{total} = \frac{3 f_v}{2 \pi r^2} \quad (13)$$

Given the assumption that all particles apply the maximum pinning force, F_{max}, the total pinning pressure exerted by the particle distribution per unit area of the boundary is:

$$P_s = N_{interact} F_{max} = \frac{3 f_v \gamma}{2 r} \quad (14)$$

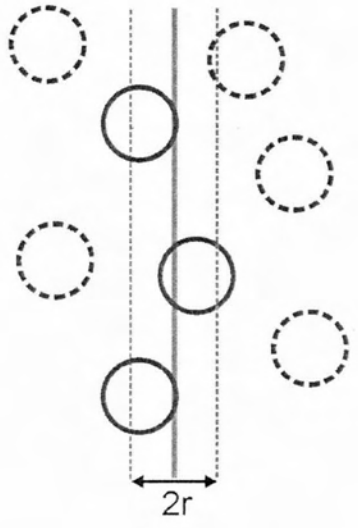

Figure 5: **Schematic of the particles that can intersect a planar boundary within one radius (solid circles).**

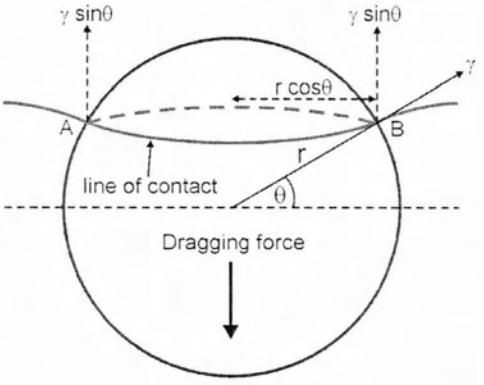

Figure 6: **Schematic of the interaction a boundary and a particle.**

This may be a significant pressure if the particles are fine. Anisotropic particles may have a larger effect if they present a greater surface area for interaction with the boundary.

This is referred to as the Zener pinning pressure. It follows that large pinning pressures are produced by:

- Increasing the volume fraction of particles
- Reducing the particle size

The Zener pinning pressure is orientation dependent, which means that the exact pinning pressure depends on the amount of coherence at the grain boundaries.

A grain of radius r has a volume $\frac{4}{3}\pi r^3$ and surface area $4\pi r^2$. The grain boundary energy associated with this grain is $2\pi r^2\gamma$ where γ is the boundary energy per unit area and we have taken into account that the grain boundary is shared between two grains. If follows that:

energy per unit volume $= \frac{3\gamma}{2r} \equiv \frac{3\gamma}{D}$, where D is the grain diameter

It is this which drives the growth of grains with an equivalent pressure of about 0.1 MPa for typical values of γ=0.3 Jm^{-2} and D=10μm. This is not very large so the grains can readily be pinned by particles (Zener drag).

An Example: The micrographs below are from a steel sample of chemical composition Fe-0.06C-0.3Si-1.02Mn-0.2Cu-2.43Ni-0.2Cr-0.46Mo wt%, containing a variety of oxygen concentrations. The oxygen is in the form of fine oxide particles. The sample was metallographically polished and then heated to 1200°C to thermally etch the austenite grain boundaries. The oxide particles serve to prevent the growth of austenite grains during this heat-treatment, via Zener pinning. It is not surprising that the final austenite grain size decreases as the oxygen concentration increases (Fig. 7).

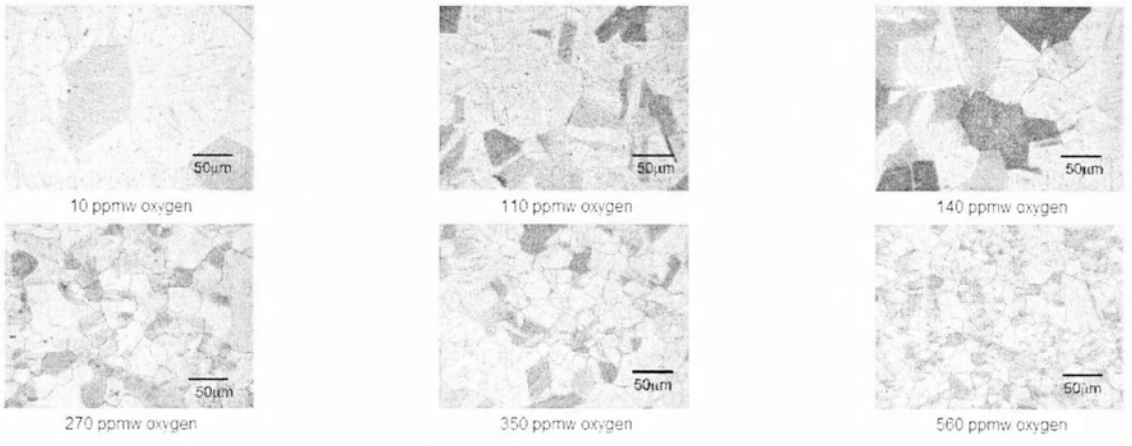

Figure 7: **Micrographs of a steel sample containing oxygen concentrations on the form of fine oxide particles.**

Computer Simulation of the Pinning force

Particle pinning has been studied extensively with computer simulations. Monte Carlo and phase field simulations have been used in 3D to model the phenomenon. Complex shape of interface can be captured in the computer models. It can provide better approximation for the pinning force.

2.4 Phase Field Model

The phase field method has proved to be extremely powerful in the visualisation of the development of microstructure without having to track the evolution of individual interfaces, as is the case with sharp interface models. The method, within the framework of irreversible thermodynamics, also allows many physical phenomena to be treated simultaneously. Phase field equations are quite elegant in their form and clear for all to appreciate, but the details, approximations and limitations which lead to the mathematical form are perhaps not as transparent to those whose primary interest is in the application of the method.

Imagine the growth of a precipitate which is isolated from the matrix by an interface. There are three distinct quantities to consider: the precipitate, matrix and interface. The interface can be described as an evolving surface whose motion is controlled according to the boundary conditions consistent with the mechanism of transformation. The interface in this mathematical description is simply a two–dimensional surface with no width or structure; it is said to be a sharp interface.

In the phase–field method, the state of the entire microstructure is represented continuously by a single variable known as the order parameter ϕ. For example, $\phi = 1$, $\phi = 0$ and $0 < \phi < 1$ represent the precipitate, matrix and interface respectively. The latter is therefore located by the region over which ϕ changes from its precipitate–value to its matrix–value (Fig. 8). The range over which it changes is the width of the interface. The set of values of the order parameter over the whole microstructure is the phase field. A two phase microstructure and the order parameter ϕ profile is show on a line across the domain (Fig. 9). Gradual change of order parameter from one phase to another shows diffuse nature of the interface.

The evolution of the microstructure with time is assumed to be proportional to the variation of the free energy functional with respect to the order parameter:

$$\frac{\partial \phi}{\partial t} = \mathrm{M} \frac{\partial g}{\partial \phi} \qquad (15)$$

where M is a mobility. A functional g(φ) has to be developed.

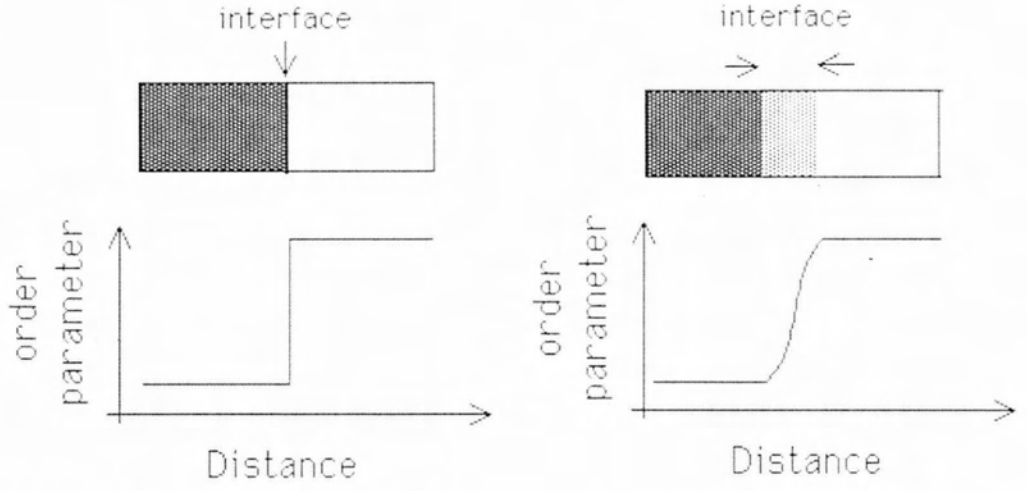

Figure 8: **a) Sharp interface, b) Diffuse interface**

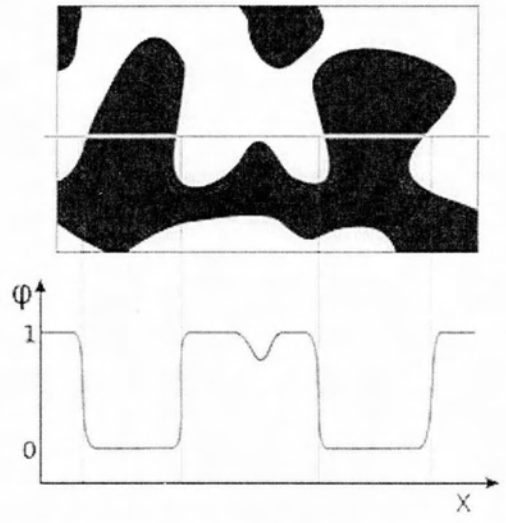

Figure 9: **A two phase microstructure and the order parameter ϕ profile is shown on a line across the domain. Gradual change of order parameter from one phase to another shows diffuse nature of the interface.**

A Taylor expansion for a single variable about X = 0 is given by:

$$J\{X\} = J\{0\} + J'\{0\}\,\frac{X}{1!} + J''\{0\}\,\frac{X^2}{2!}\ldots \tag{16}$$

A Taylor expansion like this can be generalised to more than one variable. Cahn assumed that the free energy due to heterogeneities in a solution can be expressed by a multivariable Taylor expansion:

$$g\{y,z,\ldots\} = g\{c_0\} + y\frac{\partial g}{\partial y} + z\frac{\partial g}{\partial z} + \ldots + \frac{1}{2}\left[y^2\frac{\partial^2 g}{\partial y^2} + z^2\frac{\partial^2 g}{\partial z^2} + 2yz\frac{\partial^2 g}{\partial y \partial z} + \ldots\right] + \ldots \tag{17}$$

in which the variables, y, z, . . . in our context are the spatial composition derivatives (dc/dx, d^2c/dx^2, etc). For the free energy of a small volume element containing a one–dimensional composition variation (and neglecting third and high–order terms), this gives:

$$g = g\{c_0\} + \kappa_1 \frac{dc}{dx} + \kappa_2 \frac{d^2c}{dx^2} + \kappa_3 \left(\frac{dc}{dx}\right)^2 \tag{18}$$

where c_0 is the average composition and

$$\kappa_1 = \frac{\partial g}{\partial (dc/dx)}$$

$$\kappa_2 = \frac{\partial g}{\partial (d^2c/dx^2)} \tag{19-21}$$

$$\kappa_2 = \frac{1}{2} \frac{\partial^2 g}{\partial (dc/dx)^2}$$

In this, κ_1 is zero for a centrosymmetric crystal since the free energy must be invariant to a change in the sign of the coordinate x. The total free energy is obtained by integrating over the volume:

$$g_T = \int_V \left[g\{c_0\} + \kappa_2 \frac{d^2c}{dx^2} + \kappa_3 \left(\frac{dc}{dx}\right)^2 \right] \tag{22}$$

On integrating the third term in this equation by parts:

$$\int \kappa_2 \frac{d^2c}{dx^2} = \kappa_2 \frac{dc}{dx} - \int \frac{dk_2}{dc} \left(\frac{dc}{dx}\right)^2 dx \tag{23}$$

The first term on the right is zero, so that an equation of the form below is obtained for the free energy of a heterogeneous system, the term g describes how the free energy varies as a function of the order parameter; at constant T and P, this takes the typical form:

$$g = \int_V \left[g_0\{c,T\} + \in (\nabla c)^2 \right] dV \tag{24}$$

$$g = \int_V \left[g_0\{\phi,T\} + \in (\nabla \phi)^2 \right] dV \tag{25}$$

where V and T represent the volume and temperature respectively. The second term in this equation depends only on the gradient of ϕ and hence is non–zero only in the interfacial region; it is a description therefore of the interfacial energy. The first term is the sum of the free energies of the precipitate and matrix, and may also contain a term describing the activation barrier across the interface.

Advantages

1. Particularly suited for the visualisation of microstructural development.
2. Straightforward numerical solution of a few equations.
3. The number of equations to be solved is far less than the number of particles in system.
4. Flexible method with phenomena such as morphology changes, particle coalescence or splitting and overlap of diffusion fields naturally handled. Possible to include routinely, a variety of physical effects such as the composition dependence of mobility, strain gradients, soft impingement, hard impingement, anisotropy etc.

Disadvantages

1. Very few quantitative comparisons with reality; most applications limited to the observation of shape.
2. Large domains computationally challenging.
3. Interface width is an adjustable parameter which may be set to physically unrealistic values. Indeed, in most simulations the thickness is set to values beyond those known for the system modelled. This may result in a loss of detail and unphysical interactions between different interfaces.
4. The point at which the assumptions of irreversible thermodynamics would fail is not clear.
5. The extent to which the Taylor expansions that lead to the popular form of the phase field equation remain valid is not clear.
6. The definition of the free energy density variation in the boundary is somewhat arbitrary and assumes the existence of systematic gradients within the interface. In many cases there is no physical justification for the assumed forms. A variety of adjustable parameters can therefore be used to fit an interface velocity to experimental data or other models.

Software based on Phase Field Models:

- PACE3D - Parallel Algorithms for Crystal Evolution in 3D is a parallelized phase-field simulation package including multi-phase multi-component transformations, large scale grain structures and coupling with fluid flow, elastic, plastic and magnetic interactions. It is developed at the Karlsruhe University of Applied Sciences and Karlsruhe Institute of Technology.
- The Mesoscale Microstructure Simulation Project (MMSP) is a collection of C^{++} classes for grid-based microstructure simulation.
- The Microstructure Evolution Simulation Software (MICRESS) is a multi-phase field simulation package developed at RWTH-Aachen.
- The OpenPhase is the open source software project targeted at the phase field simulations of complex scientific problems. The core of the library is based on the multiphase field model. The project has the form of a library and is written in object oriented C++. The development of the library is done by the group of Prof. Dr. Ingo Steinbach at the Interdisciplinary Centre for Advanced Materials Simulation (ICAMS).

2.5 Micress Software

MICRESS is the software used in the current paper to simulate the recrystallization and grain growth of an Aluminium Alloy. The software MICRESS (MICRostructure Evolution Simulation Software) is developed for time- and space-resolved numerical simulations of solidification, grain growth, recrystallisation or solid state transformations in metallic alloys. MICRESS covers phase evolution, solutal and thermal diffusion and transformation strain in the solid state. It enables the calculation of microstructure formation in time and space by solving the free boundary problem of moving phase boundaries. Microstructure evolution is governed essentially by thermodynamic driving forces, diffusion and curvature. In case of multicomponent alloys, the required thermodynamic data can either be provided to MICRESS in the form of locally linearised phase diagrams, or by direct coupling to thermodynamic data sets via a special TQ interface, developed in collaboration with Thermo-Calc™ AB, Stockholm.

MICRESS is based on the multiphase-field method which defines a phase-field parameter for each phase involved. The phase-field parameter describes the fraction of each phase as a continuous function of space and time. Each single grain is mapped to a distinct phase- field parameter and is treated as an individual phase. A set of coupled partial differential equations is formed which describes the evolution of the phase-field parameter, together with concentration, temperature, stress and flow fields. The total set of equations is solved explicitly by the finite difference method

on a cubic grid.2D and 3D simulations are possible. The size of the simulation domain, the number of grains, phases and components is restricted mainly by the available memory size and CPU speed. Scope of this reference is to review the current state of the art with respect to simulation of microstructure evolution based on the phase-field approach in technical alloy grades. Starting from a short overview about computational thermodynamics and kinetics and respective databases for technical alloys, an engineering approach to phase-field and multiphase-field models will be depicted in order to allow for a basic explanation of these methods -in general being developed by physicists and mathematicians- for materials scientists and metallurgists.

Binary and ternary phase diagrams being available in printed form in books or publications have provided the basis for the development of materials ever since. Increasing availability of computers has allowed for the continuous development of computational thermodynamics and respective databases in the last decades.

Such software tools and databases are nowadays available for complex alloy systems comprising a number of alloy elements, e.g. Thermo-Calc, Pandat, FactSage, JMatPro. Their databases are established using a well-defined assessment scheme (Calphad).They allow determining phase diagrams, calculating the sequence of phase transitions, the amount of phase fractions being stable at a given temperature and other thermodynamic properties, fig.10. Even more important for describing the evolution of a microstructure is that such models also allow the calculation of the driving forces for the phase transformations.

Continuing from the knowledge about equilibrium phase fractions –which do not provide any information about how fast this equilibrium is reached –subsequent developments aimed at describing the kinetics of diffusion controlled phase transitions. One example for a software tool especially suitable for the description of multicomponent diffusion using respective databases is DICTRA. The underlying approach here is based on 1-D systems like e.g. diffusion couples, concentric cylinders or concentric spheres. Under some specific assumptions phenomena like coarsening of a precipitate distribution can also be tackled.

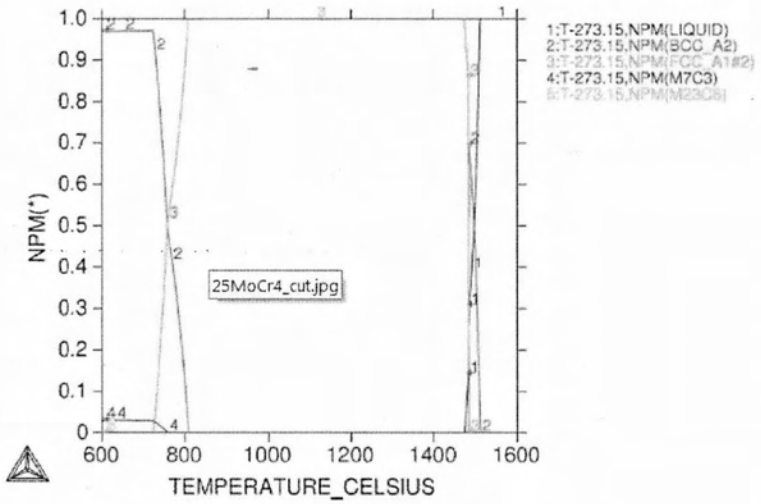

Figure 10: **Equilibrium phase fractions of different phases in a 25MoCr4 steel as a function of temperature (calculated using Thermo-Calc and the TCFe6 database)**

Most interesting for metallurgists and materials engineers, however, is the microstructure and –even further– the properties of a material being based on its microstructure. The simulation of microstructures in technical alloy systems probably has its origin in the first dendrites being simulated using the phase-field method [33] and the subsequent extension of the phase- field method

to multiple phase-fields [34] allowing early simulations of eutectic and peritectic systems. This multiphase-field model later has been coupled to thermodynamic and mobility databases, thus providing the basis for all the examples on simulations of technical alloy grades being depicted in this paper. For reviews of these developments the reader is referred to [35], [36], [37] and [38].

The phase-field method can be rigorously derived from thermodynamic principles and theories of phase transitions, and a lot of dedicated literature is available covering these fundamental and mathematical aspects (for a review see e.g. [39], [40]). In this paper it is given a phenomenological approach for a rather intuitive interpretation of the phase-field concept and equations.

The first step towards the simulation of the dynamics of microstructure evolution is the basic description of a static microstructure, fig.11. A simple approach is to use a so called order parameter ϕ for simulations of microstructure evolution in a simple solid/liquid system. ϕ itself is a function of space x and time i.e. $\phi=\phi(\vec{x},t)$ and may take values between 0 and 1. Metallurgists may relate this order parameter to the fraction of a specific phase (e.g. ϕ corresponds to the fraction solid in fig. 11) to be present at a specific point of space x and at a specific time t.

This method of describing microstructures has been extended to the description of multiple grains and multiple phases in the multiphase-field method,where multiple, i.e. "i" different phase fields $\phi_i=\phi(\vec{x},t)$ denote the individual phases or even all deferent grains. In short, any object which can be identified in the microstructure may have its own phase-field variable in respective multiphase-field models.

Before entering multiphase-field models it seems wise to understand or at least to get a feeling for a description of the evolution of the simple solidification situation depicted in fig.11. Describing the evolution of the microstructure thus means to identify the time derivative of the $\phi(\vec{x},t)$ i.e. $\dot{\phi}(\vec{x},t)$.

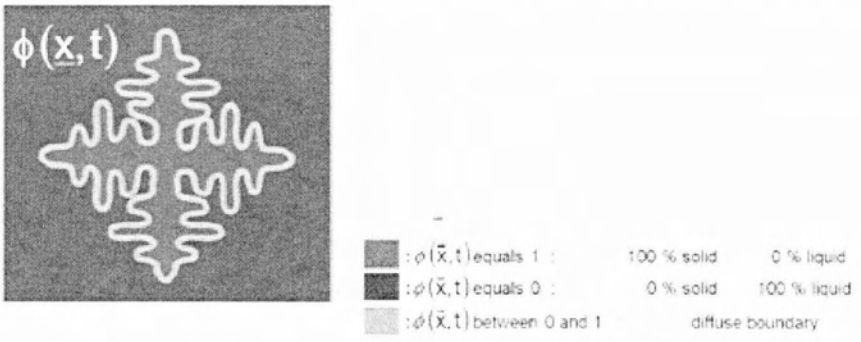

Figure 11: **Description of a solidifying microstructure by an order parameter at a given moment t. The color coding is explained above.**

A possible first step towards identification of a description of $\dot{\phi}(\vec{x},t)$ is to start from a diffusion equation (fig.12, blue contribution). A pure diffusion approach however would lead to a smear out of an initially sharp interface eventually ending up with a smooth and flat curve. In order to describe a stable, stationary interface an additional term thus is needed (fig. 12, green contribution), which stabilizes the interface. Note that this contribution is negative for $0<\phi<0.5$ and positive for $0.5<\phi<1$. This term thus balances the effect of the diffusion term (blue) leading to a stationary, stabilized interface profile. Depending on the actual choice of this term, different stationary interface profiles may result (e.g. a hyperbolic tangent profile for a double well potential or a sine–profile for a double obstacle potential). Eventually any deviation from equilibrium (fig.12, red contribution) will lead to a movement of the stationary Interface profile. The deviation from equilibrium is characterized by $\triangle G$. Depending on the sign of $\triangle G$ the motion will result either in growth or shrinkage of the respective phase. When equilibrium is reached ($\triangle G=0$) the profile characterizing the interface position will become stationary and stable. Further variables

in the respective equation denote the interfacial energy (σ), the interfacial thickness (η) and the interfacial mobility (μ):

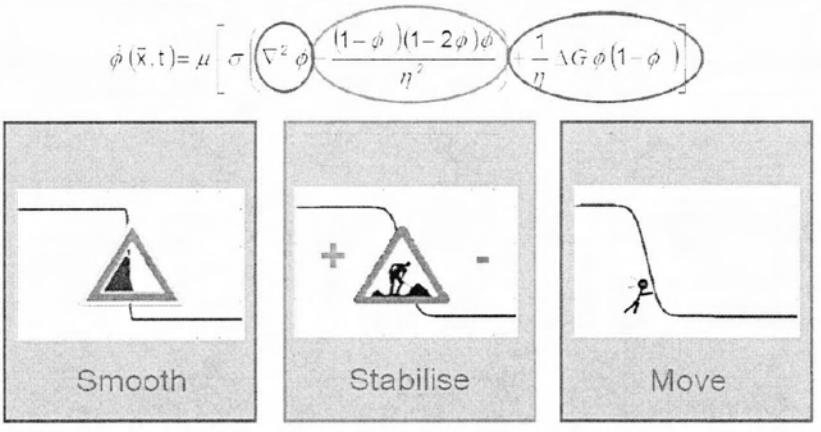

Figure 12: **The phase-field equation in a very simple analysis. See text for explanation of the individual.**

Another engineering approach to the phase-field equation is based on the "Gibbs Thomson equation" giving a relation between interface velocity, thermal and solutal undercooling and interface curvature and being well known to metallurgists since decades [41], [42].

A closer look at the phase-field equation (equation in fig. 12) reveals a rotational symmetry as the diffusion equation (fig. 12, blue contribution) does not comprise any anisotropy. In order to include anisotropy into the model, both the interfacial energy σ and the interface mobility μ are assumed to be anisotropic. In 2 dimensions this can be accomplished by making these parameters dependant on the angle θ between the growth direction and the crystal orientation i.e. $\sigma = \sigma(\theta)$ and $\mu = \mu(\theta)$. For a simple cubic symmetry in 2D these functions could look like $\sigma=\sigma_0(1-\cos(4\theta))$ and $\mu = \mu_0(1-\cos(4\theta))$. For a hexagonal symmetry in 2D functions like $\sigma=\sigma_0(1-\cos(6\theta))$ and $\mu = \mu_0(1-\cos(6\theta))$ would represent a first approach.

In case f spatially varying interfacial energies the Gibbs-Thomson coefficient Γ has to be modified by including the second derivative of the interfacial energy:

$$\Gamma = \frac{\sigma}{L_0 T_m} \quad \text{turns into} \quad \Gamma = \frac{\sigma - \sigma''}{L_0 T_m} \tag{26}$$

In order to describe anisotropy in 3D configurations a more complicated description becomes necessary.

The driving force ΔG depends on local conditions of external fields like temperature T or concentration c_i of the i different alloy elements (but also: stresses/strains, electric/magnetic fields, ...): $\Delta G = \Delta G(T, c_i)$. A non-vanishing ΔG will lead to a finite change in phase fraction i.e. a finite $\dot{\phi}(\vec{x}, t)$. This change in phase fraction in turn will affect the external fields (fig. 13). Thus there is a need of solving the coupled system of partial differential equations for the phase-field (in multiphase-field models: the multiple phase fields) and for all external fields affecting the phase transition.

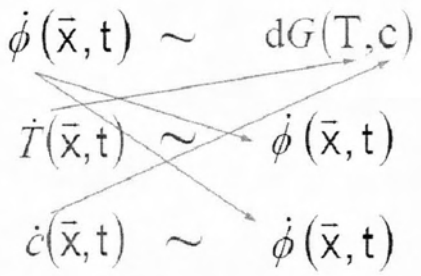

Figure 13: **Evolving phase fractions influence e.g. the temperature field T by the release of latent heat or the concentration fields ci due to the segregation of solute. These changes in turn alter the local conditions for the driving force dG.**

Technical alloys comprise multiple grains, multiple phases and multiple components. Their description in numerical models requires at least the introduction of multiple phase fields, the description of multicomponent diffusion and thermodynamic and kinetic data. The basic ideas of the multiphase-field approach [33] are:

- Definition of one phase field for each phase and for each grain of a phase
- Pairwise interaction for each pair of phases/grains like in standard phase-field
- Possibility of implementation of specific phase boundary/grain boundary properties

Further conceptual aspects comprise coupling to concentration fields [43] use of thermodynamic databases resp. mobility databases, multiphase interactions and physics of triple junctions.

Basic model development

Starting from the initial idea of describing microstructure evolution in multiphase systems [34] a number of further developments was necessary to make the model applicable and useful for technical alloy systems. The respective major topics are shortly outlined in the following and the reader is referred to respective articles for further reading.

In detail – amongst others - the following topics have continuously been addressed since 1996:

- aspects of multiphase equilibria
- sharp interface asymptotics
- aspects of computational efficiency
- coarsening phenomena
- coupling to concentration fields including solute diffusion
- consideration of fluid flow
- coupling to thermodynamic databases
- incorporation of nucleation phenomena
- incorporation of elasticity/plasticity
- self-consistent coupling to macroscopic simulations

Grain growth

Phase-field models do not always require an explicit thermodynamic driving force to drive the evolution of a microstructure. Because the respective equations can be derived from the Gibbs-Thomson relation, they implicitly tend to minimize curvature and thus allow for the description of ripening and grain growth. Subsequent to models for ideal grain growth], effects of particle pinning on the mobility of the grain boundaries have been included, fig. 14. Respective models now allow for the description of abnormal grain growth, e.g. during case hardening or for the description of grain growth in microalloyed line-pipe steels.

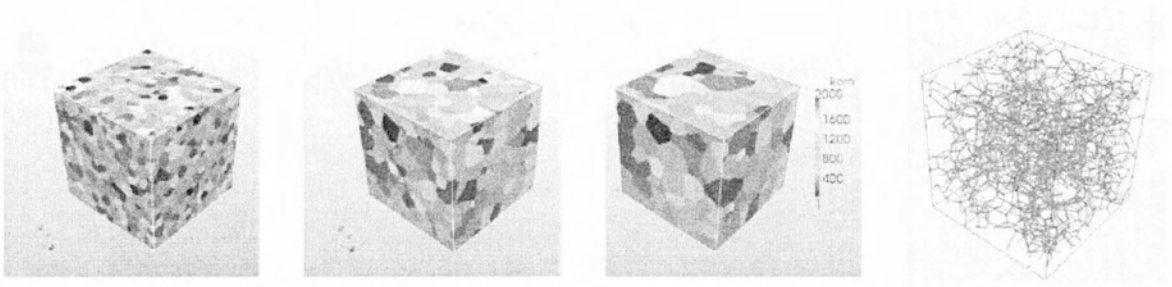

Figure 14: **3D grain growth simulation for different time steps starting from 2000 individual grains. Color coded are the individual grains (left). On the right: representation of the triple lines of intersecting grain boundaries.**

2.6 Similar Work

This paper concerns the recrystallization and grain growth of an Aluminium Alloy 5-xxx (Al.Mg-Sc-Zr) based on a Phase-Field Model. There are not any other similar papers on this topic. Although there have been made some experiments on strengthening mechanisms of an Al-Mg-Sc-Zr alloy [44] and on the influence of the particle size on recrystallization and grain growth in Al-Mg-X (where X is Mn, Zr or Sc) alloys [45].

3. METHODOLOGY

In order to "Run MICRESS" the user has to go along with the structure of an input file required for a MICRESS simulation. The numerical simulation of real processes such as microstructure evolution requires mathematical models that describe the existing physical ones. MICRESS solves the so-called Stefan problem with a modified Gibbs-Thomson relation to model microstructure evolution. The solution of the mathematical problem of e.g. solidification involves process and material parameters, description of initial conditions, nucleation criteria, definition of the calculation domain as well as the consideration of some numerical parameters for PDE solvers. The phase-field method is used by MICRESS as a numerical approach to the Stefan problem.

By now, the phase-field method is the most appropriate numerical approach for bridging the length scales between the interface capillarity length of a few nanometres and the millimetre scale of diffusion. The main characteristic feature of the phase-field model is the diffusiveness of the interface between two phases. The interface is described by a steep but continuous transition of the phase-field variable(x,t) between two states. However,technical alloys consist of multiple grains, multiple phases and multiple components. Their description requires among others the introduction of multiple phase fields, description of multicomponent diffusion and coupling to thermodynamic databases. Some of the basic ideas of the multiphase-field approach are:

- definition of one phase field for each phase and for each grain of this phase
- pairwise interaction for each pair of phases/grains similar to the standard phase field
- possibility of implementation of specific phase/ grain boundary properties
- optional use of higher order interactions in triple or multiple junctions

Further concepts of the multiphase field approach are the coupling to thermodynamic databases and the coupling to mobility dataases.
In order to obtain reasonable simulation results, MICRESS performs time loops among the nucleation model, the multiphase-field solver, multicomponent diffusion solver and the temperature solver. Coupling to thermodynamic database yields information about the nucleation undercooling, the driving force, the solute partitioning, the diffusion matrix, latent heat, etc. The obtained information is necessary for the different solvers in order to be able to perform the corresponding calculations for each time loop.

The input file / driving file
MICRESS requests input data from the terminal by a read statement. This input contains all the necessary information to start a simulation.

It can be read from a text file, the so called driving file, via a shell or directly from keyboard. The driving file has the extension "*.dri" or "*_dri.txt".
The MICRESS input data is given in a sequential form with the input file divided into several sections. Their function and meaning will be explained in the following lines. Below each section it follows the exact input file for the simulation concerning this paper. The input parameters inserted in the input file are summarized in Table 1.

Type of coupling	phase		
Time input data	Time [sec]	270	
Phase data	1 distinct solid phase		
	recrystallization		
	anisotropy		
	cubic		
Grain input	from file		
	Recr. Energy [J/cm^3]	3.0, 5.0	
	Rotation angle	25°	
		interface	triple
Data for further nucleation	max # of new nuclei	50,100	75,150
	grain radius [µm]	0.61	0.91
	Critical Recry. Energy [J/cm^3]	2.8	2.5
Phase interaction data	Surface energy [J/cm^2]	1.08*10^{-4}	
	Kinetic coefficient [cm^4/Js]	3.8*10^{-5}	
	Critical Curvature [1/µm]	0.3, 0.7, 0.9, 1.3, 1.7, 2.1	
	Minimal mobility [cm^4/Js]	0.0	
Boundary conditions	Initial temperature [K]	723.15	

Table 1: **Input parameters inserted in the input file.**

Language settings

The user can choose between English, German and French language options. When running the input file, all text outputs are generated in the language selected by the user.

```
# Language settings
# ==================
# Please select a language: 'English', 'Deutsch' or 'Francais'
English
#
```

Geometry

The input begins with the dimension and the numerical resolution of the simulation domain, i.e. the user has to specify the number of numerical grid cells in each direction and the grid spacing. In this context, the user decides whether to perform a 1D, 2D or a 3D simulation. The grid spacing is specified in micrometers. It is one of the most important numerical parameters as it determines the numerical resolution. The grid resolution should be high enough to resolve the diffusion profiles, depending on the diffusion coefficients and the growth velocity of the interface, and the curvatures of the finest expected microstructures. As an optional parameter, a rescaling factor for the graphical outputs can be given. Then, the outputs are written with a correspondingly smaller resolution. The simulation itself is not affected by this parameter.

```
# Geometry
# --------
# Grid size?
# (for 2D calculations: AnzY=1, for 1D calculations: AnzX=1, AnzY=1)
# AnzX:
450
# AnzY:
1
# AnzZ:
400
# Cell dimension (grid spacing in micrometers):
# (optionally followed by rescaling factor for the output in the form of '3/4')
0.500
#
```

Flags

Type of coupling

In the "Flags" section the type of coupling to be used for the numerical approach has to be specified. The option "phase" means that the pure phase-field model will be used with no coupling to other fields. The choice is best e.g. for grain growth simulations in pure, polycrystalline phases, as in the current simulations. Another option is "concentration". If "concentration" is selected, concentration-field coupling will be performed. This option is the most common used for the analysis of alloys. This option has better results in case thermodynamic data is available. Although in the Thermo-Calc there is available a database including both Zr and Sc elements, in the DICTRA software there is not an available database concerning the phases that would be used in the simulations of this paper, so there are not any kinetic data available for the MICRESS to be used.

```
# Flags
# -----
# Type of coupling?
# Options: phase concentration temperature temp_cyl_coord
#          [stress] [stress_coupled] [flow]
phase
#
```

Type of potential

The user can select either "double_obstacle" or "multi_obstacle. The option multiobstacle especially comprises corrections for triple junction terms and is important for correct wetting characteristics.

```
# Type of potential?
# Options: double_obstacle multi_obstacle [fd_correction]
double_obstacle
#
```

Phase field data structure

In this section, the initial dimensions for the internal fields iFace and nTupel must be specified. During runtime, the size of these fields is determined automatically, so in most cases the given values are of minor importance. The values have go be given relative to the size of the simulation domain, a value of 1.0 for iFace for example would assume that the whole calculation domain could be covered by (two-grain or two-phase) interfaces without exceeding the given initial list size. The same holds for nTupel and the coverage of the domain with triple or higher junctions. The actual usage for both fields can be found in an output file, the .TabL .

The arrays iFace and nTupel are fully dynamic, so the influence of the initial values is quite limited. In extreme cases, the specification of excessively high initial values can lead to a memory overflow during the program startup. Too low values can lead to an unnecessarily high number of reallocation steps which slow down the initialisation process e.g. in the case of grain growth simulation with a high number of initial grains. Initial values of 0.1 for both parameters are recommended and work in practically all cases.

```
# Phase field data structure
# -------------------------
# Coefficient for initial dimension of field iFace
#  [minimum usage] [target usage]
0.1
# Coefficient for initial dimension of field nTupel
#  [minimum usage] [target usage]
0.1
#
```

Restart options

MICRESS allows the user either to start a new simulation ("new") or to restart from the last output of an old one ("restart"). The "restart" option thus gives the possibility to continue a stopped simulation or to start various simulations (e.g. for a parameter variation) from a common starting point defined by a previous simulation. Thus, calculation time and effort can be saved. Even if the restart option is used, all input parameters have to be specified like for a new simulation run. Those parameters which represent initial conditions like initial composition and temperature are replaced automatically by the values from the restart file.

```
# Restart options
# ===============
# Restart using old results?
# Options:   new      restart [reset_time]
new
#
```

Selection of the outputs

In this section, the types of output files which shall be written by MICRESS must be specified. These outputs are either binary files which can be viewed with DP_MICRESS (unless another format is specified explicitly in the "Name of output files"section), or text files which can be opened with standard text editors. Traditionally, each output type has to be activated or deactivated in an extra line in the driving file and in the requested order by using the corresponding positive or negative keyword, e.g. "out_restart" or "no_out_restart"for writing or not writing a restart file.

```
# Name of output files
# ====================
# Name of result files?
Results_Grain_Growth_with_pinning/Grain_Growth_with_pinning
# Overwrite files with the same name?
# Options:   overwrite     write_protected     append
#            [zipped|not_zipped|vtk_zipped|vtk_not_zipped]
#            [unix|windows|non_native]
overwrite
#
# Selection of the outputs
# ========================
# [legacy|verbose|terse]
```

```
#
# Restart data output?                    ('rest')
# Options:   out_restart    no_out_restart      [wallclock time, h.]
no_out_restart
# Grain number output?                    ('korn')
# Options:   out_grains     no_out_grains
out_grains
#
etc.
```

Time input data

The times for user-defined intermediate outputs can be specified in this section. For convenience, the user should include an early output time in order to check whether the simulation has started correctly. Series of outputs with a constant interval or factor between the times can be easily defined with 'linear_step' or 'logarithmic_step' (for geometric series). Then, the time step for the phase-field solver has to be defined. The total time is 4.5 minutes.

```
# Time input data
# ===============
# Finish input of output times (in seconds) with 'end_of_simulation'
# 'regularly-spaced' outputs can be set with 'linear_step'
# or 'logarithmic_step' and then specifying the increment
# and end value
# ('automatic_outputs' optionally followed by the number
#  of outupts can be used in conjuction with 'linear_from_file')
linear_step 0.1 5
linear_step 1 20
linear_step 5 100
linear_step 10 270
end_of_simulation
# Time-step?
# Options: (real)  automatic [0<factor_1<=1] [0<=factor_2] [max.] [min.]
# (Fix time steps: just input the value)
automatic
# Coefficient for phase-field criterion 1.00
# Number of iterations for initialisation?
5
#
```

Phase data

This section begins with an input of the number of solid phases which will be used in the simulation. Phase number 0 is the "background" or "matrix" phase which is implicitly defined and which is assumed to be isotropic (liquid). In this paper there is only one phase, the FCC. The contribution of the $Al_3(Sc,Zr)$ phases is inserted into the simulation as a pinning force, which will be explained below. Then, for each phase specific properties have to be defined. First, the user has to specify whether a stored energy will be defined for this phase and whether recrystallisation will be included into the simulation. Then, the type of anisotropy for each solid phase has to be specified as "isotropic", "anisotropic", "faceted" or "antifaceted". If the choice is not "isotropic", further information on the crystal symmetry is required, as in this input file where "anisotropic" is selected.

The different growth shapes of crystals are a consequence of their atomic lattice structure which results in orientation-dependent interface energies and kinetics. The most common type of anisotropy

is the cubic metallic anisotropy which in the 2D case is represented by a 4-fold cosine function. The anisotropy formulation of the interface energy and mobility used for "metallic anisotropy" in 2D is:

$$x=x0*(1-k*\cos(n*)) \quad (27)$$

where x is the energy or mobility, k is the static or kinetic anisotropy coefficient, n depends on the symmetry (n=4 for cubic, n=6 for hexagonal symmetry), and is the relative orientation of the interface normal to the anisotropic grain.

If the faceted or antifaceted models are chosen, each facet orientation has to be specified explicitly. This requires the specification of all individual normal vectors of the facets in the local coordinate system. If the specified symmetry is not "none", then the individual normal vectors of the facets are mirrored further, according to the chosen symmetry. Normal vectors in opposite direction are treated as equivalent.

Furthermore, one has to specify the parameter kappa, which defines the sharpness of the anisotropy function. The antifaceted model is a recently implemented inverse faceted anisotropy function which can be used for needle-like growth.

Next, the user has to decide whether to use grain categorization. This option allows for sorting the grains of each phase in a user-defined number of orientation "categories". Using categorization, simulations can be sped up, as some operations in MICRESS are quadratic with respect to the number of grains (or categories). The "categorize" keyword here means that you want to assign grains with identical properties (including orientation) to the same grain number for a given phase. No additional parameter is required after the keyword "categorize".

Finally, the user has to decide in which way grain orientations shall be specified through the rest of the input file. The options are as one angle in 2D ("angle_2D"), as a 3D Euler notation ("euler_zxz"), as one rotation angles plus a corresponding axis ("angle_axis") or as Miller indices "miller_indices").

```
# Phase data
# ==========
# Number of distinct solid phases?
1 : FCC
#Al-Mg matrix phase
#
# Data for phase 1:
# -----------------
# Simulation of recrystallisation in phase 1?
# Options: recrystall no_recrystall
recrystall
# Is phase 1 anisotrop?
# Options: isotropic anisotropic faceted antifaceted
anisotropic
# Crystal symmetry of the phase?
# Options: none xyz_axis cubic hexagonal
cubic
# Should grains of phase 1 be reduced to categories?
# Options: categorize no_categorize
no_categorize
#
# Orientation
# -----------
```

```
# How shall grain orientations be defined?
# Options:   angle_2d
#          euler_zxz
#          angle_axis
#          miller_indices
angle_2d
#
```

Grain input

In this section, the microstructure at the beginning of the simulation needs to be specified. The input begins with determining the type of grain positioning. The initial grain structure can either be specified explicitly grain by grain ("deterministic"), by stochastic means ("random") or by reading in a file which represents the initial geometry of the grains ("from_file").

A general rule during grain input is that grain numbers are chosen automatically in a consecutive manner. Grains with a higher number can erase those with lower number if they completely cover them. In case of a partial overlap, the overlapping region by default belongs to the grain with a higher number. Only if the "Voronoi" option is chosen, the overlapping region is distributed between the grains by use of the Voronoi construction. If a grain radius is defined which is smaller than the grid resolution x, a grain consisting of only one interface cell is created which has a grain fraction corresponding to the 3D volume specified by the radius. For those grains, no reasonable curvature can be evaluated using the normal phase-field equation. Therefore, an alternative curvature treatment has to be defined. The "stabilisation" model neglects the curvature as long as the grain is still small. In the "analytical_ curvature" model, curvature is calculated from the phase fraction, assuming a spherical morphology. In this case an extra critical radius has to be defined, which determines the maximum value of the curvature for this grain.

If a particle is smaller than the numerical interface thickness, the phase-field algorithm is not suitable to evaluate the correct curvature of the particle. This is a problem for nucleation, because new grains upon nucleation are typically much smaller than the typical microstructure length scale. Inoculants which are often added to commercial alloys for grain refinement are usually much smaller than the numerical interface thickness (< 1m). If after nucleation the grain diameter (grains are assumed to start growing on a spherical seeding particle with the same radius) is much smaller than the grid spacing, the grains are treated using an analytical expression for the curvature. The "analytical curvature" feature uses a full equivalent curvature instead of the phase-field curvature.

As already explained, using the "stabilisation" feature, a reduced curvature is assumed at a given stage instead of the phase-field curvature. When the "stabilisation" option is used, the curvature term is neglected until a sufficient size is reached and curvature can be turned on continuously. Typically, the central cell of the new grain needs at least a fraction larger than 0.5 to be able to be grown by the phase-field algorithm (for triple junctions it may be more complicated). In MICRESS, the curvature increases linearly with the fraction of the central cell, i.e. the full curvature is experienced not before the grain reaches "full size" (the central cell has a fraction larger than 1-phMin).

The stabilisation option assumes a growing seed. If the critical radius is larger than the grid spacing, the seed will neither grow nor vanish, i.e. it is metastable because of the artificial curvature reduction. This stabilisation may be terminated by using the "kill_metastable" flag. To avoid this situation (due to a very small grid spacing, high interfacial energy or small stored energy), the option "analytical_curvature" should be used.

If there are no grains to be present at the beginning of the simulation, the user should specify "deterministic" and define the number of grains at the beginning as 0. In this case, no additional input is necessary in this section.

Deterministic

With this option, first the number of grains at the beginning has to be specified. For each grain, the geometry (round, rectangular or elliptic) and the grain positioning is defined by Cartesian coordinates with the origin at the bottom left-hand corner (in 2D simulations, only the x and z coordinate hasto be given). Round grains are defined by their radius, rectangular and elliptic grains by the length along the x and the z-axis. If round grain geometry has been chosen, the curvature model which is to be used in case of small grains has to be specified. Furthermore, the user has to specify whether in case of overlapping grains the Voronoi construction is to be used and which phase number is associated with the grain. Depending on the properties of this phase, the recrystallisation energy and the orientation of the grain has further to be given.

random

For random grain positioning, an integer for randomization is required as first input. Essentially, this "random seed" assures reproducibility of the initial grain structure when other parameters of the input file are changed. Afterwards, the number of different types of grains has to be specified. By the different types it is possible to e.g. define complex size distributions or to fill different zones of the simulation domain with grains of different size or geometry. For each grain type, the number of grains and the grain geometry must be specified. As in the case of deterministic grain positioning the user can define round, rectangular or elliptic grains. Furthermore, a minimum and a maximum value are required for each-space coordinate in order to define the region over which the grains of this type shall be randomly redistributed. Depending on the type of the geometry chosen, the user has to further specify a minimum and a maximum radius (round geometry) or a minimum and a maximum length size along each-axis (rectangular or elliptic geometry) in order to define the size distribution of the actual grain type.

In the same way as for deterministic input, the curvature model which is to be used in case of small grains has to be specified (if a "round" geometry has been selected), the user has to specify whether the Voronoi construction is to be used, which phase number is associated with the grain of the actual type and, depending on the phase properties, the recrystallisation energy has further to be given. Additionally, a minimum distance between the grains (in μm) is required. This parameter, besides the minimum and maximum radius, helps to avoid overlapping of grains. In Voronoi construction, this parameter is helpful to obtain equal size distributions.

from_file

In case of reading the initial grain structure from file, first its name and path needs to be specified. For defining the initial grain structure, an image file in ASCII format is required. The geometry of this file has to be given as AnzX and AnzZ (for 2D simulations).These dimensions have not necessarily to be the same as the dimensions of the simulation domain specified at the top of the input file. There have been written two inputs files with different initial microstructure, $\tilde{S}_1 > \tilde{S}_2$ where $\tilde{S}_i$ is the average grain surface of each microstructure.

Comparing the three methods of the initial grain structure the third is the best, while the user can insert the exact microstructure of the alloy.

```
# Grain input
# ===========
# Type of grain positioning?
# Options: deterministic  random  from_file
from_file
# File for grain properties
Microstructure_400_320.txt
# Treatment of data?
# (n: none, 1: 1D, f: flip (bottom<->top), t: transpose,
#  or p: 'phase to grains transformation')
```

```
fp
# AnzX for initial microstructure?
400
# AnzZ for initial microstructure?
320
# Number of grains at the beginning?
# (Set to less than 1 to read from input data,
#  with optionally a minimal size, in cells)
-1
#
```

The number of grains at the beginning can be either specified explicitly or read from the input file. If the grain properties for the defined number of grains are specified in an extra file, its name and path has to be given.

Otherwise, the grain properties are read in directly from the command line. They can be set to "identical", i.e. all grains have the same properties, or they can be read as blocks. The latter would mean grain 1 to 3 and grain 4 to 6 if the number of grains was set to 6. In this specific simulation there is one type of grains whose recrystallization value is 3.0 J/cm^3 and the rotation angle is 25°. The recrystallization energy is the stored energy of the alloy. In order to compare the influence of the stored energy there has been writen another input file with the value of the recrystallization energy to be 5.0 J/cm^3.

```
# Read grain properties from a file?
# Options:  input   from_file   identical   blocks
identical
# Input data for grain number 1:
# Phase number?  (integer)
1
# Recrystallisation energy?
3.0000
# Rotation angle? [Degree]
+25.0000
# 'Non-geometric' data for grains 1 to 108 identical
#=====================================================
```

Data for further nucleation

There are different nucleation models used by MICRESS which refer to different types of phases or circumstances where nucleation is to occur. These are for example a specific interface, in the bulk or phase regions. Moreover, it is important to know whether a fixed critical undercooling or some other criteria based on the seeding particle properties, stored energies in recrystallisation, etc. shall be used as a nucleation criterion. The user specifies which phase is nucleated on which substrate phase and in which phase the solutal undercooling of the nucleating phase is calculated (matrix phase). The user also determines the temperature range, the checking frequency, data for shielding subsequent nuclei, etc.
The following nucleation models are implemented in MICRESS:

seed density model

The seed density nucleation model implemented in MICRESS is based on a heterogeneous nucleation model similar to the one used by Lindsay Greer [46].

During heat extraction from the melt, the largest particles will nucleate first at an undercooling defined by their radius (if complete wetting is assumed or an effective radius is used instead). The particles start growing and releasing latent heat, while interacting with other potential nucleation precursors. Depending on the heat extraction rate and the amount and dimensions of all other seeding particles, the temperature will drop more or less below the liquidus temperature, thus defining the amount of seeds to be activated. According to the model, the effectiveness of inoculants added for grain refinement is defined by:

- the maximum particle size
- the particle size distribution

In MICRESS, the seed density model should be used together with latent heat or with coupling to the one-dimensional temperature field (1d_temp) in order to allow an interaction of the potential nucleation sites via release of latent heat, but sometimes it may seem appropriate to use it just as a simple way to randomly distribute a given number of nuclei in a defined region.

Particularly, the model describes nucleation from the melt, triggered by small seeding particles which may be added intentionally or which may exist as impurities. Essentially, the critical undercooling for nucleation of a given phase on this seeding particle depends on the radius of the seeding particle and the surface energy of the new phase in the liquid. Consequently, if a radius-density distribution of the seeding particles is known, depending on the cooling conditions, the model can predict how many nuclei will be formed.

If the different grains of the new phase grow competitively, like in equiaxed solidification, the latent heat released by the growing particles has to be taken into account. The easiest temperature boundary condition. Thus, the total amount of latent heat is released globally on the whole simulation domain.

At the beginning of the simulation, for all seed types which use the seed density model, discrete positions with discrete radii for the potential nucleation sites are determined and stored. During the simulation run, nucleation is checked only at these predefined places. These seeding particles are not "consumed" by nucleation and cannot move. An exception is the "moving_frame" option in the section "boundary conditions": If this option is selected, the predefined nucleation sites move with the frame, the sites which move out at the bottom of the domain are copied to the top line in order to keep the density of nucleation sites constant. If "seed_density" is selected, the user first has to specify an integer for randomization. The random number generator has to be initialized with an arbitrary integer number.

In the seed density model, the size distribution of potential nucleation sites (seeding particles) is described in terms of classes with different radii [µm] and density [cm^{-3}].

For each class, the number of potential nucleation sites is calculated according to the given density and the volume of the simulation domain.

Using the given density, explicit positions of the potential nucleation sites are determined. The radii (and thus the local critical undercooling for nucleation on each particle) are distributed evenly according to the radius range of each seed class. Inside each class, a random radius distribution is assumed. The radius range corresponds to the radius difference to the next specified class. The finally created numbers and radius ranges for each class can be found in the log-file.

The seed classes must be specified starting with the highest radius values. At least two classes should be specified, otherwise the automatically assumed radius range may lead to unexpected results.

seed undercooling model

Using the seed undercooling model, a new seed is set if the local undercooling at a nucleant position exceeds a predefined critical nucleation undercooling, as in the current simulations. The local undercooling is depending on the local composition and temperature.
In general, the MICRESS nucleation models are designed for micro-scale simulations and not for the nano-scale, i.e. there is no model for the prediction of homogeneous nucleation based on thermal fluctuations for the critical seed formation.

In praxis, inoculants are often added to technical alloy melts which serve as nucleation agents during solidification. They help to achieve a smaller grain size and to suppress columnar growth. Even if no active inoculation is done, impurities, dislocations or the roughness of the interface structures can lead to nucleation phenomena in all types of technical processes. Unfortunately, apart from the "seed density model" for heterogeneous nucleation from an inoculated melt, no physical models are available for the complex nucleation conditions in technical alloys. Homogeneous nucleation, on the other hand, will typically occur only at very high undercooling and under extremely clean conditions, like in experiments with levitated drops.

Thus, besides the physically based "seed density model" for heterogeneous nucleation, MICRESS provides the user with a pragmatic nucleation model based on a critical undercooling which can be further specified with respect to the type of seed positioning, the temperature range, the matrix and substrate phases, the nucleation rate etc. and which allows the user to mimic the complex nucleation circumstances found in technical alloys or processes. All these parameters can be specified in the section "Data for further nucleation".

The keyword "nucleation" activates nucleation input. The option "out_nucleation" in the next line gives the possibility to obtain additional graphical result outputs for the time-step when nuclei are set or a phase disappears. Next, the number of types of seeds must be specified. By using several seed types, different nucleation conditions can be independently defined for different phases on different types of positions, for different temperature intervals etc.

In contrast to the seed density model, no explicit potential nucleation sites are predefined and the number of grains which can nucleate during simulation is not limited. Therefore, the user can specify a maximum number of grains which are allowed for each seed type. In the input files comparing the average grain surface, as mentioned above, the number of new nuclei is bigger in the input file with the finer microstructure. Grain boundaries are good sites for nuclei to form. Since a decrease in grain size results in more boundaries this results in an increase in the nucleation rate.

Next, an explicit radius for the grains of this type has to be specified. If a value higher than the spatial discretisation x is chosen, then a grain with the corresponding size and a sharp interface is created.

If a value lower than the spatial discretisation x is chosen, a „small" grain consisting of only one interface cell is created. Usually, a value of 0 will be used to start with the smallest possible fraction of 2 x phMin (see section „Other numerical parameters"). By this way, any kind of concentration imbalance is avoided (given that phMin has been chosen appropriately).

Under certain circumstances, the user may wish to specify a radius value between 0 and x. Then, a grain consisting of a single cell with a fraction of the new phase corresponding to the 3D volume will appear. Afterwards, the small grain model to be used must be specified.

The minimum undercooling specifies at which undercooling nuclei are allowed to form. This undercooling is calculated using the local composition (if concentration coupling is used),

temperature and, if applicable, the local curvature of the substrate phase. In case of recrystallisation, the value of the stored energy is used instead.

After having chosen the nucleation model to be used in the simulation, the orientation of the new grains has to be specified, if the phase of the new phase has not been set to isotropic (phase input data). A random distribution, a fix value, an orientation range or a parent relation, i.e. a relative orientation to the grain of the local substrate phase, can be chosen. The last option applies only to nucleation at interfaces or junctions. Then, the shield data have to be specified. Shielding means that no further grain of the same phase will be nucleated during the shield time within the shield distance of a previously nucleated grain. No categorisation will be applied to this grain during the shield time (otherwise the shield properties would be lost). The shield time is also used by the "kill_metastable" option, no killing is performed during the shield time.

The shield time and the shield distance parameters are related. They account for a physical shield effect due to the release latent heat or solute by a new grain which is not explicitly included in the simulation. This allows the user to set up a pragmatic nucleation scenario if the exact physical background is unknown. Supposed that at a time t a nucleus appears, the parameter "shield distance" will define a circular area with the diameter r shield around the grain. No other grains of the same phase will be allowed to appear on this area within the time interval (t, t+tshield). The r shield parameter can be defined according to experimental micrographs of the system to be simulated and tshield can be evaluated e.g. according to some typical diffusion time scale considerations.

In case of the seed density model, explicit shielding is not compatible with the underlying physical model. The user is requested to specify only a "shield time"which still is necessary to control the categorisation and „kill_metastable" functions.

If in section „phase data", „categorize" and „anisotropic" have been chosen for the nuclei phase, the user has to decide whether for this seed type categorisation of the orientation values to orientation categories shall be performed. This is important, if different grains shall be assigned to the same grain number during run-time, because this is only possible if all grain properties including orientations of the grains are identical. After the keyword „categorize", the number of orientation categories can be specified, default is 36 (corresponding to 10° difference between the orientation categories in 2D).
Further, MICRESS requests a minimum and a maximum nucleation temperature for the actual seed type. A minimum and maximum temperature should be chosen around the temperature where nucleation is expected. The parameters primarily help to minimize unnecessary nucleation checks and thus to improve performance.

In a first trial, it is wise not to restrict the nucleation range. The time between checks for nucleation determines the frequency of nucleation checking. If chosen too high, insufficient seeding may occur in spite of high local undercooling. If chosen too small, an unnecessarily high numerical effort and a corresponding performance loss can be the consequence.

The noise is applied as $G(1+k*(random -0.5))* G$ where k is user defined noise amplitude, $0 \leq random \leq 1$ is the value of the random number generator and ΔG is the nucleation driving force.

Input for each seed type

For each seed type, a type of positioning must be given. Seeds may be placed in the bulk (="inner" part of the grains), in regions, at interfaces, at triple or at quadruple junctions. Unless the additional keyword "restrictive" is used, the choice of a given keyword includes all keywords

which in the options list are found right of this keyword. Thus, "bulk" or "region" include all interfaces, triple points and higher junctions, "interface" includes all triple or quadruple junctions and so on. If "region" is requested, the coordinate ranges in micrometer must be given in the following lines.

After that, the phase number of the new grains and the reference phase must be defined. New grains can appear only where the reference phase is present. In case of concentration coupling, the driving force for nucleation is calculated using the local composition in this phase. In solidification simulations e.g. the liquid phase is typically the reference phase.

If the "type of position" is neither "bulk" nor "region", an additional substrate phase (and an optional second substrate phase) is required for further specification of the interfaces where nucleation should occur, and for defining which of the two phases in the interface defines the curvature contribution to the nucleation undercooling (for "interface" only). This curvature contribution is disregarded if the substrate phase is identical to the reference phase.
In continuation, the nucleation model to be used for further nucleation is defined. MICRESS uses two nucleation models – the seed density model and the seed undercooling model. The seed density model is designed for heterogeneous nucleation in a melt, therefore it is only available for "bulk" or "region". In all other cases, the seed undercooling model is chosen by default. Both models will be presented separately within the next sections.

Input for all seed types

After specification of all seed types, some few inputs remain to be done which apply to all seed types. First of all, if any of the seed types is using random noise, an integer number for randomization has to be given to assure reproducibility. The maximum number of simultaneous nucleations is the number of grains of all seed types allowed to be nucleated in the same time step. A list of possible seeds is created and ordered with respect to the undercooling or driving force for each nucleus. If the maximum number is exceeded, the less favourable seeds are discarded. The option may lead to unexpected results if more than one seed type is defined and therefore should be used carefully. Setting the maximum number of simultaneous nucleations to "automatic" (=0) removes this check. In some cases, "stabilised" small grains can erroneously reach a metastable state at which they stop growing, but also do not vanish because their stabilisation implies a reduced curvature. By enabling the flag "kill_metastable", the stabilisation of small grains is removed after their shield time has elapsed. This makes sure that "metastable grains" can vanish correctly. The option "kill_metastable" is also relevant in case of categorisation, because after „killing", small stabilized grains are considered as „big" and such can be assigned to a common grain number. The "kill_metastable" flag is only relevant for small grains which use the "stabilisation" model.

```
# Data for further nucleation
# ===========================
# Enable further nucleation?
# Options:   nucleation    no_nucleation  [verbose|no_verbose]
nucleation
# Additional output for nucleation?
# Options:   out_nucleation    no_out_nucleation
no_out_nucleation
#
# Number of types of seeds?
2
#
# Input for seed type 1:
```

```
# ----------------------
# Type of 'position' of the seeds?
# Options: bulk region interface triple quadruple [restrictive]
interface
# Phase of new grains?
1
# Reference phase?
1
#
# Substrat phase [2nd phase in interface]?
# (set to 1 to disable the effect of substrate curvature)
1
# maximum number of new nuclei 1?
50
# Grain radius [micrometers]?
0.61000
# Choice of growth mode:
# Options:  stabilisation analytical_curvature
stabilisation
# critical recrystallisation energy [J/cm**3]?
2.800
# Determination of nuclei orientations?
# Options: random fix range parent_relation
random
# Shield effect:
# Shield time [s] ?
180.00
# Shield distance [micrometers]?
1.7
# Input of minimal and maximal recrystallisation energy:
# (dG contribution only if energy is 0 on one side!)
# Minimum of recrystallisation energy? [J/cm**3]
0.0000
# Maximum of recrystallisation energy? [J/cm**3]
0.0000
# Nucleation range
# min. nucleation temperature for seed type 1 [K]
630.0000
# max. nucleation temperature for seed type 1 [K]
700.000
# Time between checks for nucleation? [s]
2.00000E-02
# Shall random noise be applied?
# Options:  nucleation_noise  no_nucleation_noise
no_nucleation_noise
#
# Input for seed type 2:
# ----------------------
# Type of 'position' of the seeds?
# Options: bulk region interface triple quadruple [restrictive]
triple
# Phase of new grains?
1
# Reference phase?
```

```
1
# Substrat phase [2nd phase in interface]?
# (set to 1 to disable the effect of substrate curvature)
1
# maximum number of new nuclei 2?
75
# Grain radius [micrometers]?
0.910000
# Choice of growth mode:
# Options:  stabilisation analytical_curvature
stabilisation
# critical recrystallisation energy [J/cm**3]?
2.500
# Determination of nuclei orientations?
# Options: random  fix  range  parent_relation
random
# Shield effect:
# Shield time [s] ?
250.0
# Shield distance [micrometers]?
2.00
# Input of minimal and maximal recrystallisation energy:
# (dG contribution only if energy is 0 on one side!)
# Minimum of recrystallisation energy?  [J/cm**3]
0.0000
# Maximum of recrystallisation energy?  [J/cm**3]
0.0000
# Nucleation range
# min. nucleation temperature for seed type 2 [K]
600.0000
# max. nucleation temperature for seed type 2 [K]
750.000
# Time between checks for nucleation? [s]
2.00000E-02
# Shall random noise be applied?
# Options:  nucleation_noise  no_nucleation_noise
no_nucleation_noise
#
# Max. number of simultaneous nucleations?
# ----------------------------------------
# (set to 0 for automatic)
5
#
# Shall metastable small seeds be killed?
# ----------------------------------------
# Options:  kill_metastable  no_kill_metastable
kill_metastable
#
```

Phase interaction data

In this section the user defines the phase interaction data and the grain boundary properties. Phase interactions can be defined for all pair-wise combinations of the phases which have been included in the "phase data" section.

In the standard input sequence, the user is requested to specify all phase interaction data in a fixed order, starting with the phase pair 0/1. Phase interactions which are not used are switched off using the keyword"no_phase_interaction". No further input is required in this case. Enabling phase interactions means that one of the phases may grow or shrink on the expense of the other. On the other hand, if a phase interaction is switched off, no movement of the corresponding interfaces is possible.

This also concerns the initialisation of the interface: if such an interface is created via the initial grain setting, the interface will stay sharp even if an initialisation is requested. The partition coefficients which are necessary for diffusion through interfaces are accessed from the other phase interactions using a "constant" approximation. If e.g. interactions are defined for phases 0/1 and 0/2, a simplified description can be derived for the 1/2 interface. This description is stored for each interface cell in the moment of creation (as initial structure or from moving triple junctions) and kept constant during the further. Switching off phase interactions can greatly reduce the complexity of a simulation, especially if many phases are included. In case of solid state reactions, only the interactions of the precipitations with the matrix and not the interactions between different types of precipitates should be included. If two contacting phases have a common stoichiometric component without solubility range, the interaction between these two phases must be switched off.

When the interaction of one phase with itself is enabled, solid-state interactions between grains of the same phase will be activated. In this case, no chemical driving force is included and the movement will be controlled only by curvature and by stored energies in case of recrystallisation.

The option "phase interaction" can be followed by an optional keyword which selects special interaction models:

"standard": this is the default interaction

"particle_pinning": enables a mesoscale model for particle pinning. If this keyword is selected, an effective mobility model is used which includes the pinning effect of not explicitly resolved particles. As further input, a critical pinning force and a minimal mobility will be requested later in this section. This is the model by which the phases $Al_3(Sc,Zr)$ contribute to the simulation.

The term "particle pinning" describes the effect of small particles on the movement of grain boundaries. If the driving force for the movement of the grain boundary (typically the curvature) is not high enough to overcome the attractive interactions with the particles, the grain boundary is "pinned" and will not move any more. Thus, the grain size may be reduced to a much lower value by the effect of particle pinning. In practice, particle pinning is an important mechanism in preventing softening of materials at high temperature due to grain growth. The particle pinning model implemented in MICRESS is a meso-scale model which takes into account the microscopic particle pinning effect without treating the individual particles explicitly. According to the Zener model, a critical pinning force $P^* \sim 3\gamma f / r$ is defined, where γ is the particle surface energy, f is the "particle concentration" and r the particle radius (Fig. 15).

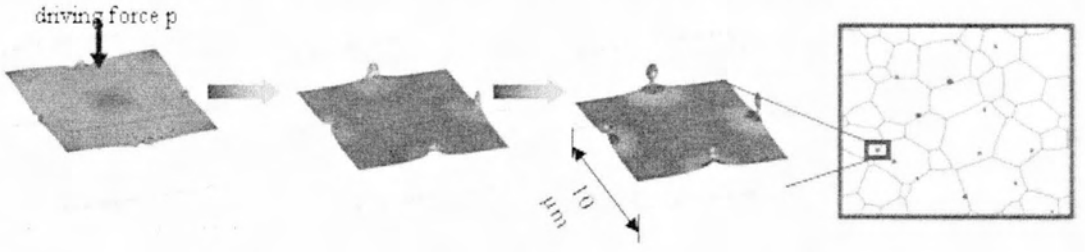

Figure 15: **The particle pinning model.**

If the driving force p exceeds the critical driving force, the grain boundary will still move, but with a lower velocity. This velocity has been simulated for discrete particles using MICRESS (Fig. 14). The velocity curves can be described by an effective mobility which is implemented in the mesoscopic MICRESS particle pinning model. The user has to provide the critical pinning force p* in units of a critical curvature (1/μm) and a minimal mobility. In order to calculate the value of the pinning force, the user has to convert the pinning force to a curvature. The curvature is:

$$P = \frac{3\gamma f}{r} = \frac{2\gamma}{\overline{D}} \Rightarrow \overline{D} = \frac{2r}{3f} \Rightarrow \frac{1}{\overline{D}} = \frac{3f}{2r} \left[\frac{1}{\mu m}\right] \tag{28}$$

According to K.L. Kendig, D.B Miracle [29] and John S. Vetrano, Steve M. Bruemmer , L.M. Pawlowski, I.M. Robertson [30] , the volume fraction of these particles is 0.015-0.035 and typical sizes range from about 50-150 nm in diameter (25-75 nm in radius). Calculating the critical curvature for the upper and lower limits:

$$\frac{1}{\overline{D}} = \frac{3f}{2r} = \frac{3*0.015}{2*75*10^{-9}} = 0.3 \left[\frac{1}{\mu m}\right]$$

$$\frac{1}{\overline{D}} = \frac{3f}{2r} = \frac{3*0.035}{2*75*10^{-9}} = 0.7 \left[\frac{1}{\mu m}\right]$$

$$\frac{1}{\overline{D}} = \frac{3f}{2r} = \frac{3*0.015}{2*25*10^{-9}} = 0.9 \left[\frac{1}{\mu m}\right]$$

$$\frac{1}{\overline{D}} = \frac{3f}{2r} = \frac{3*0.035}{2*25*10^{-9}} = 2.1 \left[\frac{1}{\mu m}\right]$$

There have been simulated seven cases concerning the value of the critical curvature, 0.0 , 0.3, 0.7, 0.9, 1.3, 1.7, 2.1 $\frac{1}{\mu m}$.

For grain growth, the driving force for grain boundary movement consists of the grain boundary curvature and the force balance at the triple junctions. In general, this driving force decreases with the average grain size. But especially the force balance at the triple junctions is not directly linked to the grain size. Therefore, with the particle pinning model, abnormal grain growth may be observed, e.g. one huge grain continues growing while the smaller ones are already pinned.

Figure 16 shows that using the particle pinning model instead of normal grain growth leads to different results. In the figure above, a clear tendency towards abnormal grain growth can be seen in the simulation where the particle pinning model has been used.

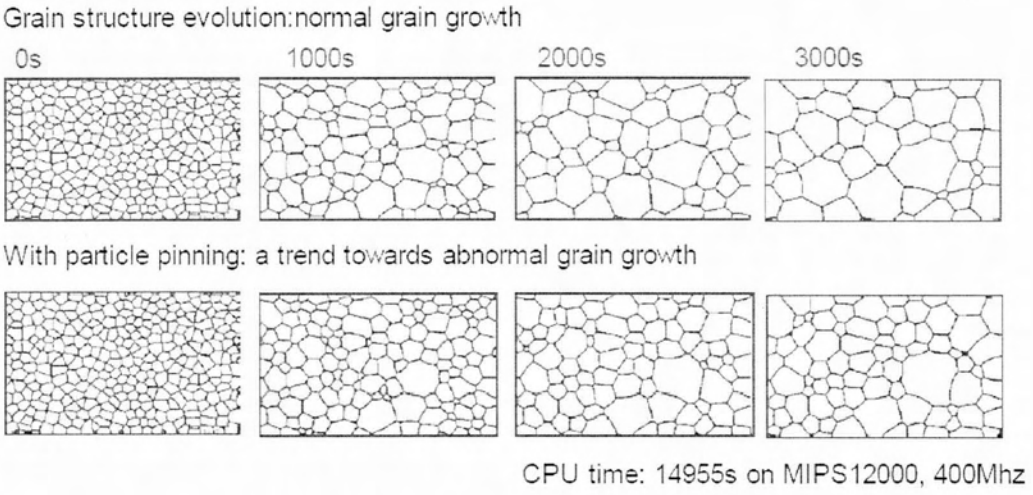

Figure 16: **Grain growth without (top) and with (bottom) the particle pinning model**

"particle_pinning_temperature": enables the mesoscale particle pining model with temperature dependent input parameters read from an ASCII file.

"solute_drag": the solute drag model is based on a two-step hysteresis description of the mobility for the "free" and "loaded" interface, as a function of the interface velocity. If this model is selected, a critical transition velocity, a transition range (for smooth transition) and a drag factor has to be specified.

The keyword "avg" is used to define an averaging of the driving force across the interface. Averaging prevents spreading of the interface if a strong concentration gradient is causing opposite driving forces on both sides of the interface. The user can specify a value between 0 (no averaging) and 1 (maximum averaging).

Averaging of the driving force helps stabilising the interface in case of diffusion controlled transformations, if the resolution is not high enough (i.e., the diffusion length is not big compared to the interface thickness). A typical value is 0.5, the default value is 0.

The keyword "max" specifies the maximum driving force allowed (value above which the driving force will be cut-off). This value is useful to shrug off some temporary problems during initial transients or to reduce the impact of numerical fluctuations. The value should be chosen high enough in order not to limit kinetics during normal growth. If a too small value is chosen for the maximum allowed driving force, the movement of the interface can be drastically slowed down.

The "smooth" keyword has only effect if averaging is specified: The gradient direction along which averaging of the driving force is performed, is randomly rotated with the specified maximum value in degrees. Depending on other circumstances, this option may help to reduce the effect of grid anisotropy on the growth morphology. A typical value is 45, default is 0.

The interface energy, which scales the effect of curvature, can be given either as a constant value (keyword "constant") or defined as "temperature_dependent". Interface energies have to be specified in J/cm^2. The value of the interface energy for an Al-alloy according to bibliography is $1.08*10^{-4}$ J/cm^2.

One of the most important phase interaction parameter is the interface mobility which defines the interface velocity for a given driving force or curvature. The mobility may be defined as constant, temperature dependent or driving force dependent. In the both latter cases, the user will be asked to provide the name of a text file where the kinetic coefficient (second column) is given in tabulated form as a function of temperature or driving force. Otherwise, just a constant value in cm^4/Js is required. According to bibliography the kinetic coefficient is $3.8*10^{-5}$ cm^4/Js. In case of some special models (solute drag, particle pinning), additional model parameters have to be included here, as the critical pinning force [1/μm] and the minimal mobility [cm^4/Js]. From a theoretical point of view, the minimal mobility parameter should be zero. But in many cases, even if pinning occurs, still a very slow movement of the grain boundaries is observed, e.g. due to particle ripening. MICRESS gives the user the possibility to account for that by specifying a minimal mobility >0.

The description of the interaction between an "anisotropic" phase and an "isotropic" one also includes a flag for the anisotropy, and if this is switched on, the static and the kinetic anisotropy coefficients have to be specified. For combinations of two anisotropic phases, an additional misorientation model is available. If the keyword "misorientation" is set, factors between the mobility or interfacial energy of high angle and low angle grain boundaries can be specified. It should be noted that phase 0 (usually liquid) is isotropic by default.

```
# Phase interaction data
# ======================
#
# Data for phase interaction 0 / 1:
# ---------------------------------
# Simulation of interaction between phase 0 and 1?
# Options:  phase_interaction  no_phase_interaction
#  [standard|particle_pinning[_temperature]|solute_drag|redistribution_control]
no_phase_interaction
#
# Data for phase interaction 1 / 1:
# ---------------------------------
# Simulation of interaction between phase 1 and 1?
# Options:  phase_interaction  no_phase_interaction
#  [standard|particle_pinning[_temperature]|solute_drag|redistribution_control]
phase_interaction particle_pinning
# Type of surface energy definition between phases 1 and 1?
# Options: constant temp_dependent
constant
# Surface energy between phases 1 and 1? [J/cm**2]
1.08000E-04
# Type of mobility definition between phases 1 and 1?
# Options: constant temp_dependent dg_dependent
constant
# Kinetic coefficient mu between phases 1 and 1? [cm**4/(Js)]
3.80000E-05
# critical pinning force [1/micrometer]
0.9
# minimal mobility [cm**4/Js]
0.0
# Shall misorientation be considered?
# Optionen:  misorientation  no_misorientation
misorientation
# Input of the misorientation coefficient:
```

Modification of surface energy for low angle
boundaries
(multiplying factor to value for high angle boundaries)
1.0000
Modification of mobility for low angle
boundaries
(multiplying factor to value for high angle boundaries)
1.00000
#

Boundary conditions
In MICRESS two classes of boundary conditions are distinguished:

thermal boundary conditions

Thermal BCs have to be specified if temperature is not explicitly simulated.
- temperature vs. time
- net heat flow vs. time
- temperature gradient vs. time
- 1d-temperature field

conditions for boundaries of the calculation domain

- for the phase-field parameter
- for the concentration field
- for the 1d-temperature field, the stress field, flow field etc

This section starts with the specification of the temperature boundary condition, if neither "temperature" coupling nor "1d_temp" is chosen in section "Flags and Settings" at the top of the input file. Three alternatives are available to describe the type of temperature trend: If the flag "linear" is chosen, the number of connecting points has to be defined. Then, first the initial temperature at the bottom of the simulation domain and the initial temperature gradient in z-direction are requested. Afterwards, for each connecting point, the time the bottom a temperature and the temperature gradient in z-direction have to be specified. The temperature and temperature gradient will be interpolated linearly between these transition points. In this way, an arbitrarily complex temperature-time profile can be applied.

If the number of connection points is set to 0, only the initial temperature at the bottom, the temperature gradient in z direction and a constant cooling rate in K/s are requested. Using the flag "linear_from_file", it is also possible to read the same information from a file consisting of three columns: the time in seconds, the temperature at the bottom in Kelvin, and the gradient in Kelvin per centimetre. This allows a more compact input for complex temperature-time input data.

While the first two options always lead to linear temperature profiles in z-direction, the option "profiles_from_file" allows to read time-dependent non-linear temperature profiles from a series of ASCII data files (or from different columns of one data input file). Again, the number of connection points has to be specified, and for each of those points, the time and a file name, optionally with specification of the used columns, has to be given.

As next, the "moving frame" options have to be set. This feature is very useful for simulations related to directional solidification, as it allows the reduction to a smaller simulation domain which follows the movement of the solidification front. This option is not available for the use of latent heat without 1d temp because it is not compatible with the assumptions of the "DTA

approximation". If the flag "moving frame" is selected, the user has to select the criterion which controls the movement of the simulation domain.

Available criteria are "temperature" or "distance". In case of "temperature", a critical temperature is requested. If the temperature at the bottom falls below this value, the domain is moved in z-direction until the bottom temperature reaches the critical value. In case of a constant cooling rate, this option leads to a constant moving velocity like in a typical Bridgman furnace experiment.

If the "out_moving_frame" flag is set, a "Gesamt" (global) data file is created additionally for all selected graphical outputs.

The boundary conditions of the simulation domain have to be set for the phase-field variables, the concentration, temperature and displacement fields depending on the type of coupling which has been defined at the beginning. The MICRESS boundary conditions are defined by a text string with length 4 or 6 which represent a sequence of key characters. The characters specify the type of boundary condition- their sequential order addresses the different sides of the simulation domain (east-west-bottom top for 2D and east-west-north- south-bottom top for 3D). The following conditions are available:

insulation ("i"): The boundary cell (the first cell outside of the simulation domain) is assumed to have the same field value (e.g. phase-field variable) as its direct neighbour (the outermost cell of the domain). The name of the flag reflects the fact that no gradients and, thus, no fluxes exist between the boundary cell and its neighbour inside the simulation domain.

symmetric ("s"): defines the field value of the boundary cell to be identical to its second neighbour in the simulation domain, thus implying a symmetry plane through the centre of the outermost cells of the domain. This condition is similar to an isolation condition which is shifted by half a cell.

periodic ("p"): with this condition, the field value of the boundary cell is set to the value of the outermost cell on the opposite side of the simulation domain. Thus, objects like dendrites which touch one side are continued on the other side. The periodic condition preserves the field balance.

gradient (g): the field value of the boundary cell is extrapolated from the first and second neighbour inside the domain. The use of this boundary condition is allowed for all fields (concentration, temperature, phase-field) but not always reasonable. The gradient condition for phase-field is very useful for grain growth. If "periodic" is not suitable for any reason – the flag "g" should be the best choice for minimising the impact of the boundary condition on the grain structure.

fixed ("f"): Uses a fixed value for the boundary cell. This value is requested in an extra input line. Naturally, the "f" condition does not preserve the average of the field value. A typical application of the fixed condition for the concentration field is directional solidification with moving frame (fixed condition for top boundary).

In case of using a 1D extension of the concentration field (by selecting the "1d_far_field" option in the "Flags" section), the top boundary condition for the concentration field is automatically shifted to the top of the 1D extension!

If the option "1d_temp" has been selected at the beginning of the input file ("Flags and Settings"), at this place the boundary conditions for the 1D temperature field have to be specified. The user can select between insulation (i), symmetric (s), periodic (p), global gradient (g), fixed (f) and flux (j). While "i", "s" and "p" have already been explained above, the other conditions are either new or have further implications or a slightly different meaning:

global gradient ("g"): This condition establishes a given global temperature gradient between the actual boundary and the opposite boundary. This modified gradient condition is especially useful for coupling to external process simulation results: If temperature vs. time and the thermal gradient are known from a macroscopic process simulation (or a corresponding experiment), a time-dependent fixed "f" condition can be applied on one side of the 1D temperature field, and the "g" condition on the other side to maintain the gradient. The definition of "g" on both sides is not allowed.

fixed ("f"): The definition of this condition corresponds to that of the fixed condition for the normal simulation domain. But, not only of a fixed temperature value, but also a temperature- time profile can be read from a text file using the "from_file" option. If a constant temperature is chosen, a heat transfer coefficient is requested additionally, allowing the definition of a heat transfer condition to an external medium with fixed temperature.

flux ("j"): This condition allows the assumption of a constant or time-dependent flux [W/cm^2] as boundary condition.

After defining the boundary conditions of the 1D-temperature field, the user has to choose whether to apply constant thermo-physical data (enthalpy, heat capacity and thermal diffusivity) for this temperature field, or to specify files where these thermophysical data shall be read from as a function of temperature. All three thermodynamic quantities are read separately for the part of the 1D-temperature field which lies above and below the micro-simulation domain. This can be important if e.g. a strongly undercooled columnar dendritic front is simulated.

```
# Boundary conditions
# ===================
# Type of temperature trend?
# Options:  linear   linear_from_file   profiles_from_file
linear
# Number of connecting points?   (integer)
0
# Initial temperature at the bottom?  (real)  [K]
723.15
# Temperature gradient in z-direction?  [K/cm]
0.E+0-
# Cooling rate? [K/s]
0.0000
#
# Options:    moving_frame    no_moving_frame
no_moving_frame
# Boundary conditions for phase field in each direction
# Options: i (insulation) s (symmetric) p (periodic/wrap-around)
#        g (gradient)  f (fixed)    w (wetting)
# Sequence: E W (N S, if 3D) B T borders
iiii
#
# Unit-cell model symmetric with respect to the x/y diagonal plane?
# Options:   unit_cell_symm  no_unit_cell_symm
no_unit_cell_symm
#
#
```

Other numerical parameters

In this last section, some purely numerical parameters for the phase-field, concentration and stress solver are defined. The maximum number of concentration solving per phase-field iteration has only to be defined, if concentration coupling is used in combination with a fixed phase-field time step. An error message is given if the number is too small to be consistent with the time- step criterion of the explicit diffusion solver. This input is not required when automatic time-stepping is used.

In case of stress coupling, the convergence criteria for the iterative BiCG-stab matrix solver as well as an upper limit (maximum number) of iterations have to be defined. In the input line for the maximum number of iterations, the input of a second integer is also possible. It is set to 20 by default and specifies the maximum number of iterations allowed for achieving a good solution for quasi-static equilibrium. In most cases, the default settings are sufficient. Next, a value for the phase minimum is required. A cell with a phase or grain fraction below this value is not considered to be in the interface any more but in a bulk region (liquid or solid). In most cases, a value of 1.E-4 can be recommended.

Finally, the interface thickness (in cells) also has to be input in this section. Generally, with increasing interface thickness, the curvature evaluation of the phase-field profile is improved. On the other hand, a higher resolution is required to resolve highly curved structures, and numerical artefacts related to the finite interface thickness like "artificial solute trapping" is increased.

In case of using extremely small values for the interface thickness (<~3 cells), curvature evaluation is poor and nucleation at the interface is not working correctly anymore.

```
# Other numerical parameters
# ==========================
# Phase minimum?
1E-04
# Interface thickness (in cells)?
5.00
#
```

4. RESULTS AND DISCUSION

The alloy studied (Al-6Mg-2Sc-1Zr wt%) has one type of particles that form on the sub-micron scale which influence the recrystallization and grain growth. In the alloy containing Sc and Zr, small coherent spherical precipitates of $Al_3(Sc,Zr)$ are formed. Their influence to the alloy is inserted to the simulations via the critical curvature due to the pinning force of Zener drag. It is supposed that following the cold work, the alloy was subjected to a 'flash annealing' treatment of 4.5 min at 450°C. This served as a comparison treatment and resulted in full recrystallization in most of simulations, depending on the value of the pinning force. Typical sizes of $Al_3(Sc,Zr)$ particles range from about 50-150 nm in diameter for the heat treatments in these simulations.

There have been three types of simulations. The first one concerns the influence of the stored energy (W) as a result of plastic strain to the recrystallized volume fraction (f_{rx}). The stored energy in these particular simulations is the recrystallization energy. The values of the recrystallization energy, as mentioned above, are W_1 = 3.0 J/cm^3 and W_2 = 5.0 J/cm^3. As it is well known increasing the internally stored energy, the material is by recrystallization returned to a thermodynamically less favorable state. Comparing two different values of stored energy, as greater is the value the faster the alloy will be fully recrystallized. The influence of processing the stored energy on the recrystallization volume fraction can be seen in Figure 17. For W_1=3.0 J/cm^3 the alloy is fully recrystallized at t_1=120 sec while for W_2=5.0 J/cm^3 is at t_2=65 sec.

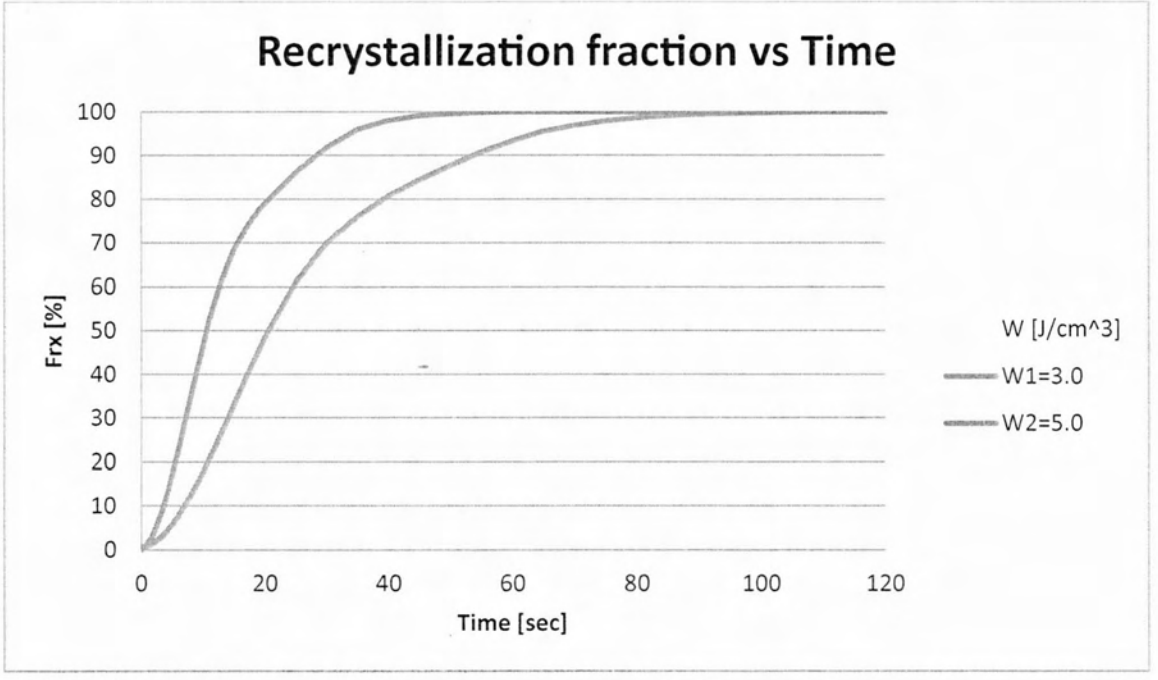

Figure 17: **Recrystallized volume fraction vs time depending on the stored energy.**

The second type of simulation refers to the influence of the average grain size of the initial microstructure. Recrystallization occurs with a clear delay at large initial grain sizes due to the low fraction of grain boundaries acting as nucleation sites. This leaves enough time for dynamic recovery to occur and its softening effect is more pronounced than in the case of small initial grain sizes. The influence of processing the initial microstructure on the recrystallized fraction can be seen in Figure 18. The recrystallized grain size does show a difference between the two initial grain sizes in these simulations. The average grain surface of each microstructure is S_1=2281,71 μm^2 and S_2=760,61

μm^2. In Figure 19, can be seen the grain size of each microstructure for time steps 0.0, 5.0, 20.0, 50.0 and 270.0 sec. At t=0 sec are the initial microstructures as inserted in the input file, as described in Appendix 1.On the left is the microstructure with the greater initial grain size ($D_1 \approx 26.96$ μm, $D_2 \approx 15.56$ μm).

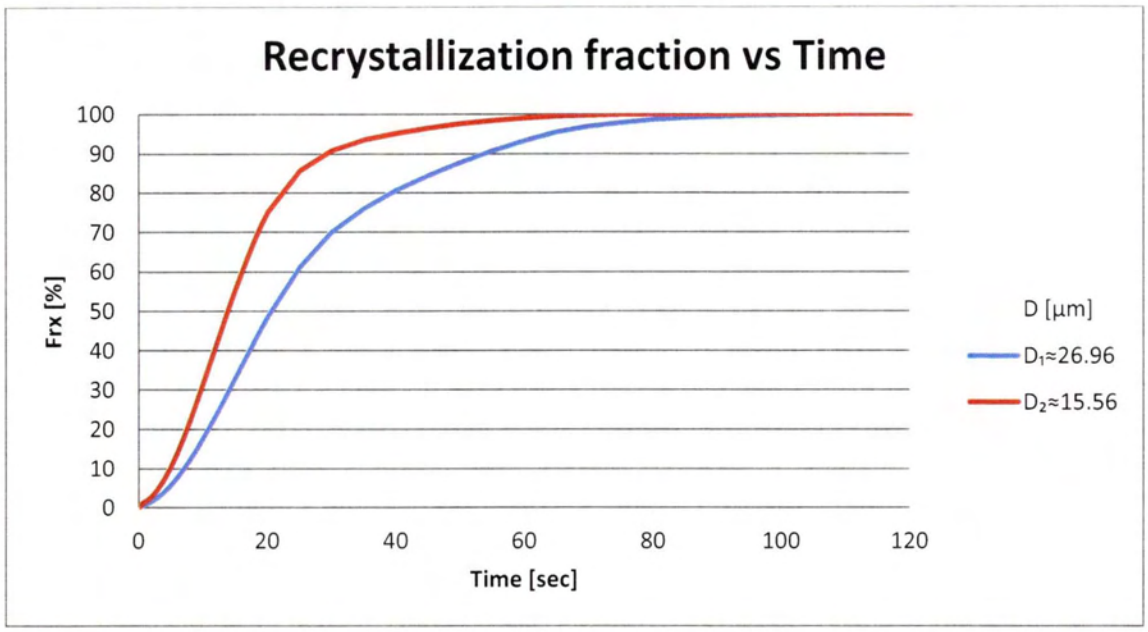

Figure 18: **Recrystallized volume fraction vs time depending on the initial grain size.**

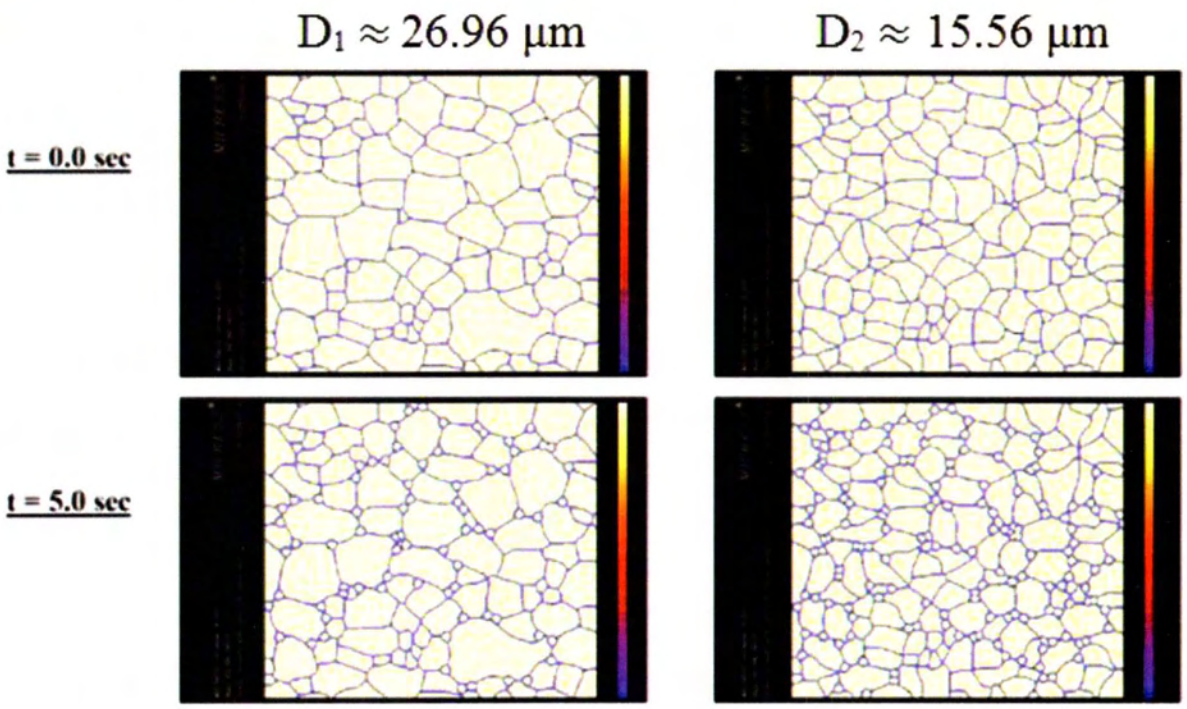

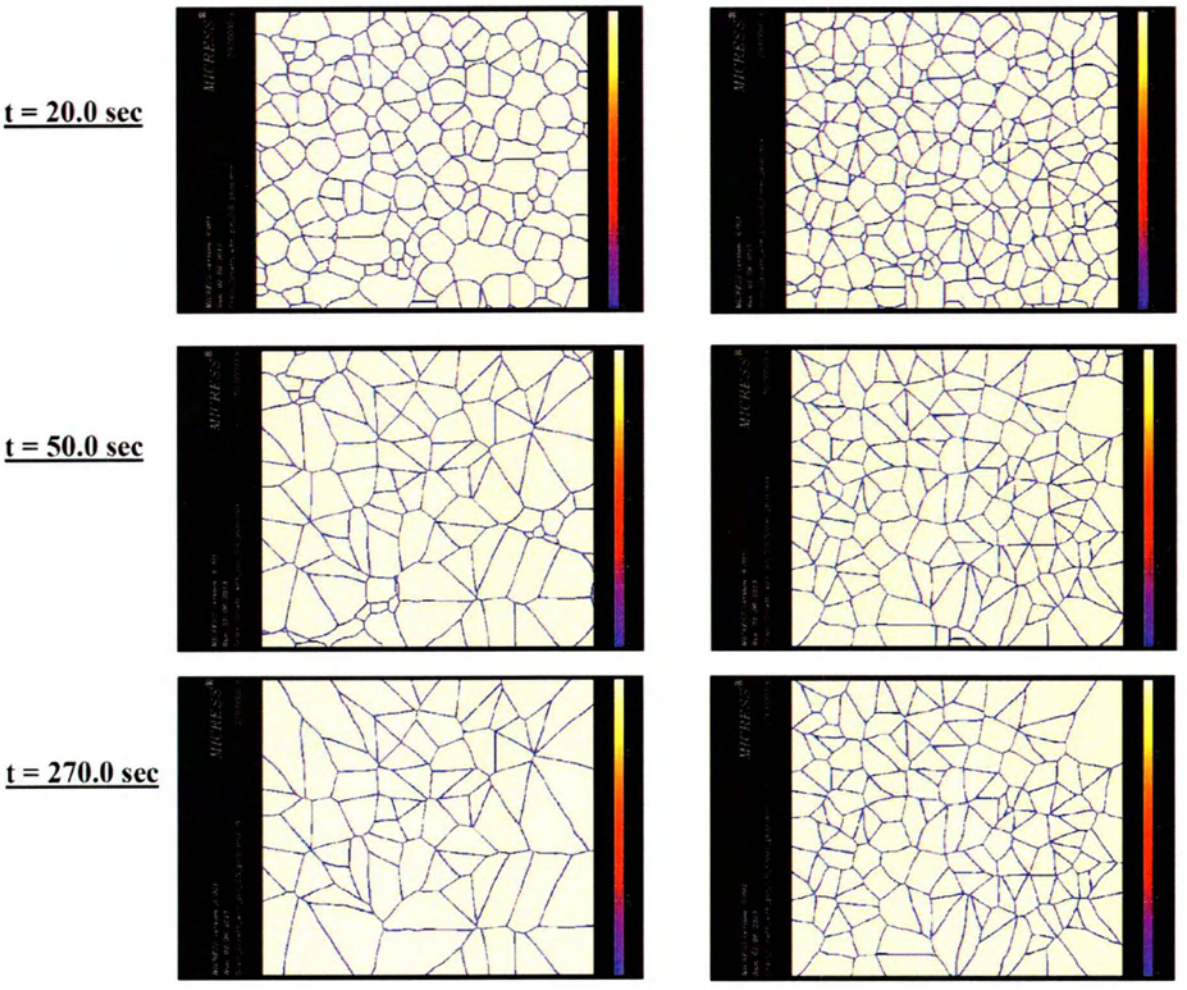

Figure 19: **The grain size of each microstructure for time steps 0.0, 5.0, 20.0, 50.0 and 270.0 sec. On the left is the microstructure with the greater initial grain size.**

The third type of simulations concerns the influence of the value of pinning force of Al_3Zr and Al_3Sc particles on the average grain radius of the alloy. Recrystallized grain size and shape are influenced by the size and density of second phase particles. Particle influence ranges from the formation of viable recrystallization nuclei to their drag on moving grain boundaries as a result of Zener pinning. This particle pinning will restrict the progression of recrystallization and contribute to a smaller average grain size. The influence of the pinning force on the final average radius is greater as its value increases, as can be seen in Figure 20. Especially it is noticeable that for finer particles (of 25nm in radius of $Al_3(Sc,Zr)$) and a greater volume fraction of these particles such as f_v=0.035 the influence of the pinning force, expressed in critical curvature $\frac{1}{\bar{D}} = 2.1\ \frac{1}{\mu m}$, is very significant on the average radius 8.9μm for t=256sec, while for $\frac{1}{\bar{D}} = 0.3\ \frac{1}{\mu m}$ the average radius is 13.82μm for t=81sec. In figure 20 the lines noticed are quite abnormal and end at different time. This is due to the output file concerning the average radius. This file is updated by default each time a grain is set or disappears, so the grain data is not available every time step.

Also the driving force for fully recrystallization is not enough to overcome the pinning force as f_{rx} = 30.62% for $\frac{1}{\bar{D}} = 2.1\ \frac{1}{\mu m}$ and f_{rx} = 100% for $\frac{1}{\bar{D}} = 0.3 - 1.7\ \frac{1}{\mu m}$ (Fig.21).

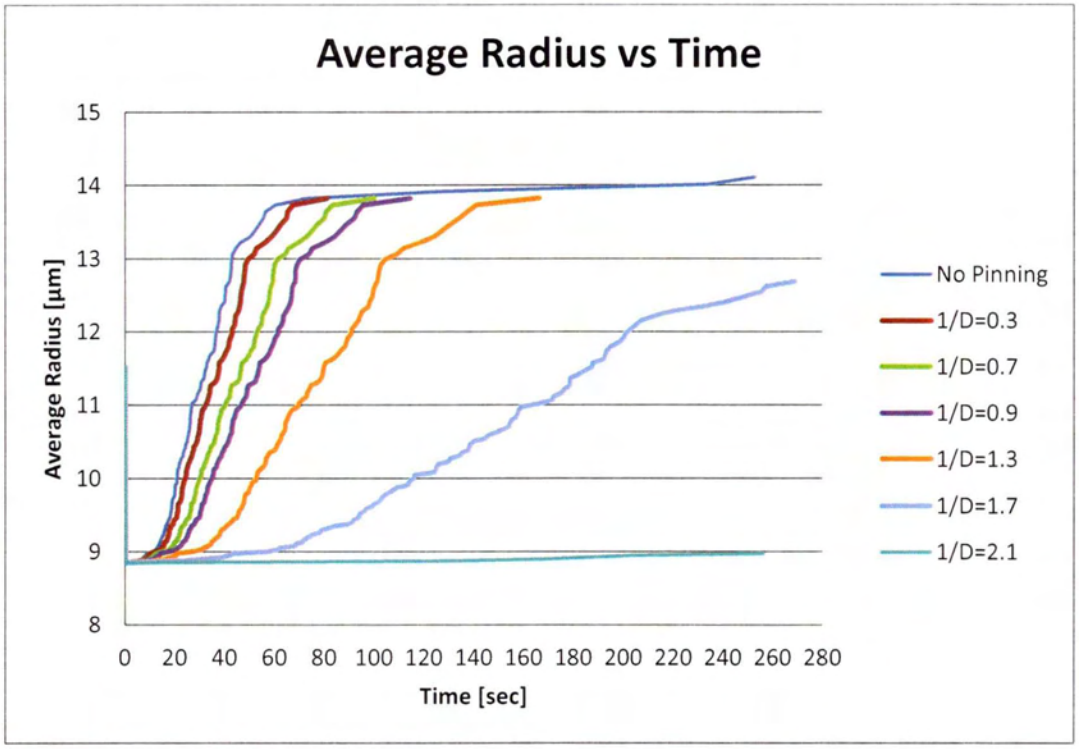

Figure 20: **Average grain size vs time depending on the pinning force.**

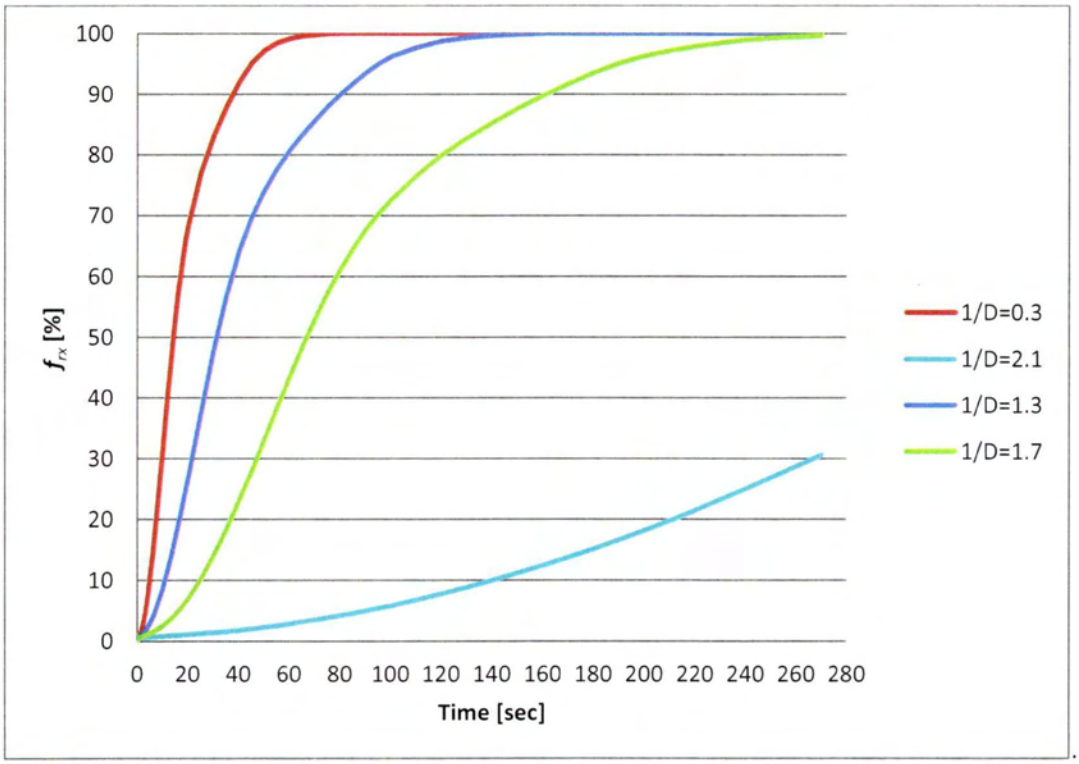

Figure 21: **Recrystallized volume fraction vs time depending on the pinning force.**

5. CONCLUSIONS

From the results presented in the previous sections the following conclusions can be drawn. The phase field method is an efficient method to simulate microstructural evolution provided an accurate set of input parameters describing the alloy system and initial conditions is provided.

Two processes have been simulated using the Micress software, recrystallization and grain growth of an Al alloy containing pinning particles of Al_3Sc and Al_3Zr. Effects of stored energy, initial grain size and pinning force were studied. It was found that:

The influence of stored energy, as shown in Figure 17, is that the alloy recrystallized more rapidly in case of greater stored energy (W_1=3.0 J/cm^3 < W_2=5.0 J/cm^3). The rate of recrystallization is influenced by the amount of deformation and, to a lesser extent, the manner in which it is applied. Heavily deformed materials recrystallize more rapidly than those deformed to a lesser extent (W_2).

The influence of initial grain size is that a finer initial microstructure, due to more grain boundaries, leads to finer final microstructure, as shown in Figure 18. Grain boundaries are good sites for nuclei to form. Since a decrease in grain size results in more boundaries this results in an increase in the nucleation rate and hence a decrease in the ratio of the recrystallized volume fraction.

The influence of pinning force is that bigger sizes of $Al_3(Sc,Zr)$ precipitates lead to finer final microstructure. The size of $Al_3(Sc,Zr)$ precipitates in Al-Mg alloys can have a marked effect on the grain morphology. The average diameter of the precipitates is 50-150 nm. With further increasing the number density f_v of $Al_3(Sc,Zr)$ precipitates, the pinning force increases evidently, while the average radius of the final microstructure is decreasing, as shown in Figure 20.

From the simulations in this work, it can be seen that the cold rolled alloy can keep partial crystallization at a temperature up to 450 °C depending on the pinning force. This confirms that $Al_3(Zr,Sc)$ precipitates have a low coarsening rate making the alloy stable at elevated temperatures. The alloy was recrystallized completely for the values of the critical curvature 0.3, 0.7, 0.9, 1.3 and 1.7 μm. However, for the value of 2.1 $\frac{1}{\mu m}$ the alloy was not fully recrystallized. The maximum recrystallization resistance comes from the simulation with critical curvature 2.1 $\frac{1}{\mu m}$ which is not completely recrystallized even at 270 sec. Such good improvement of recrystallization resistance would be related to coherent $Al_3(Zr,Sc)$ precipitates efficiently pinning the movement of dislocations and grain boundaries. The strong drag effect of these precipitates is due to the fact that they are coherent with the Al matrix and very stable thermally against loss of coherency and coarsening. Recrystallization occurs only after these precipitates have lost their coherency.

The Phase field method can be used in the future for alloy design purposes provided that accurate input parameters are provided. Based on the current work, it would be able to fulfill experiments on the Al-6Mg-2Sc-1Zr (%wt) alloy and compare the results with those derived from MICRESS simulations. As mentioned above, MICRESS requires many input parameters. After the experiments, the input parameters can be more accurate, as in this work are based on relevant published literature.

REFERENCES

[1] Sawtell RR, Morris JW. In: Kim Y-W, Griffith WM, editors. Dispersion Strengthened Aluminium Alloys. TMS Publishing; 1988. P. 40-9.

[2] L.M. Angers, D.G. Konitzer, J.L. Murray, W.G. Truckner Y.-W. Kim, W.M. Griffith (Eds.), Dispersion Strengthened Aluminum Alloys, TMS Publishing (1988), p. 355

[3] Royset J, Ryum N. Scandium in aluminium alloys [J]. Inter Mater Rev, 2005, 50(1): 19-44.

[4] Dai Xiao-yuan, Xia Chang-qing, Peng Xiao-min. Precipitation behavior of Al3(Sc,Zr) secondary particles in 7XXX aluminum alloys during annealing [J]. The Chinese Journal of Nonferrous Metals, 2010, 20(3): 451-455. (in Chinese).

[5] Dai Xiao-yuan, Xia Chang-qing, Hua Man-yu, Peng Xiao-min. Recrystallization of 7XXX aluminum alloy containing scandium [J]. Trans Mat Heat Treat, 2010, 31(1): 132-136.

[6] HE Zhen-bo, PENG Yong-yi, Yin Zhi-min, LEI Xue-feng. Comparison of FSW and TIG welded joints in Al_Mg_Mn_Sc_Zr plates [J]. Transactions of Nonferrous Metals Society of China, 2011, 21(8): 1685-1691.

[7] Booth-Morrison C, Dunand D C, Seidman D N. Coarsening resistance at 400 °C of precipitation-strengthened Al_Zr_Sc_Er alloys [J]. Acta Mater, 2011, 59: 7029-7042.

[8] Karnesky R A, Dunand D C, Seidman D N. Evolution of nanoscale precipitates in Al microalloyed with Sc and Er [J]. Acta Mater, 2009, 57: 4022-4031.

[9] Lefebvre W, Danoix F, Hallem H, Forbord B, Bostel A, Marthinsen K. Precipitation kinetic of Al_3(Sc,Zr) dispersoids in aluminum [J]. J Alloys Comp, 2009, 470: 107-110.

[10] Fuller C B, Seidman D N. Temporal evolution of the nanostructure of Al(Sc,Zr) alloys: Part II_Coarsening of Al3(Sc1_xZrx) precipitates [J]. Acta Mater, 2005, 53: 5415-5428.

[11] Seidman D N, Marquis E A, Dunand D C D. Precipitation strengthening at ambient and elevated temperatures of heat-treatable Al(Sc) alloys [J]. Acta Mater, 2002, 50: 4021-4035.

[12] Riddle Y W, Sanders T H Jr. A study of coarsening, recrystallization, and morphology of microstructure in Al_Sc_(Zr)_(Mg) alloys [J]. Metall Mater Trans A, 2004, 35: 341-350.

[13] V.G. Davydov, T.D. Rostova, V.V. Zakharov, Yu.A. Filatov, V.I. Yelagin Mater Sci Eng A, 280 (2000), pp. 30–36.

[14] Z. Ahmad JOM, 55 (2003), pp. 35–39.

[15] Y. Harada, D.C. Dunand Mater Sci Eng A, 329–331 (2002), pp. 686–695.

[16] L.Q. Chen, W. Yang Phys. Rev. B., 50 (1994), pp. 15752–15756.

[17] G.N.Haidemenopoulos, A.I.Katsamas, H.Kamoutsi Metall Mater Trans A, 2010, 41A: 888-899.

[18] D. Fan, L.-Q. Chen, S.-P.P. Chen J Am. Ceram. Soc., 81 (1998), pp. 526–532.

[19] C. Shen, Q. Chen, Y.H. Wen, J.P. Simmons, Y. Wang Scripta Mater., 50(2004), pp. 1023–1028.

[20] N. Moelans, B. Blanpain, P. Wollants Acta Mater., 54 (2006), pp. 1175–1184.

[21] N. Moelans, B. Blanpain, P. Wollants Acta Mater., 53 (2005), pp. 1771–1781.

[22] C.E. Krill, L.Q. Chen Acta Mater., 50 (12) (2002), pp. 3057–3073.

[23] Y. Suwa, Y. Saitob, H. Onodera Scripta Mater., 55 (2006), pp. 407–410.

[24] R.Doherty et al. (Drexel University, Philadelphia, USA.), Modelling and microstructure development in spray forming, vol 33, no 3, 1997, 50–60.

[25] R.W. Cahn, Internal strains and recrystallization Original Research Article Progress in Metal Physics, Volume 2, 1950, Pages 151-176.

[26] F.J. Humphreys, M. Hatherly , Recrystallization and Related Annealing Phenomena (Second Edition), 2004.

[27] J. von Neumann, J. Met. Interfaces (1952) 108.

[28] W.W. Mullins, J. Appl. Phys. 27 (1956) 900.

[29] D.A. Aboav, Metallography 3 (1970) 383.

[30] D. Weaire, Metallography 7 (1974) 157.

[31] M. Hillert, Acta Metall. 13 (1965) 227.

[32] C. Zener, cited by C.S. Smith, TMSAIME 15 (1948) 175.

[33] R. Kobayashi: "Modeling and numerical simulations of dendritic crystal growth" Physica D 63 (1993) 410-423.

[34] I. Steinbach, F. Pezzolla, B. Nestler, M. Seeßelberg, R. Prieler, G. J. Schmitz, J. L. L. Rezende: "A phase field concept for multiphase systems" Physica D 94(1996), p.135-147.

[35] I.Steinbach, B.Böttger, J.Eiken, N.Warnken, S.G.Fries: "CALPHAD and Phase-Field Modeling: A Succesful Liaison" Journal of Phase Equilibria and Diffusion 28 1 (2007) 101.

[36] T. Kitashima: "Coupling of the phase-field and CALPHAD methods for predicting multicomponent, solid-state phase transformations" Philosophical Magazine Vol. 88, No. 11, 11 April 2008, 1615–1637.

[37] S.G.Fries, B.Böttger, J.Eiken, I.Steinbach: "Upgrading CALPHAD to microstructure simulation: the phase-field method" Int.J.Mat.Res 100(2009)2.

[38] I. Steinbach: "Pattern formation in constrained dendritic growth with solutal buoyancy" Acta Materialia 57 (2009) 2640–2645.

[39] H. Emmerich:" Advances of and by phase-field modelling in condensed-matter physics" Advances in Physics 57(2008)1.

[40] U.Hecht et al.:"Advances of and by phase-field modelling in condensed- matter physics (vol 57, pg 1, 2008" Advances in Physics 59 3(2010)257.

[41] .J. Diepers, Diploma thesis, Access, RWTH Aachen 1997.

[42] C. Beckermann, H.-J. Diepers, I. Steinbach, A. Karma, X. Tong: "Modeling Melt Convection in Phase-Field Simulations of Solidification" Journal of Computational Physics 154 (1999) p. 468.

[43] J. Tiaden: "Phase field simulations of the peritectic solidification of Fe- C" Journal of Crystal Growth 198/199 (1999), pp 1275-1280.

[44] K.L. Kendig, D.B Miracle, Strengthening mechanisms of an Al-Mg-Sc-Zr alloy, 2001.

[45] John S. Vetrano a,;k, Steve M. Bruemmer ', L.M. Pawlowski b, I.M. Robertson, Influence of the particle size on recrystallization and grain growth in Al-Mg-X alloys, 1997.

[46] A.L. Greer et al., "grain refinement of aluminium alloys by inoculation," Adv Eng Mater, 5 Mater 2003, 81.

APPENDICES

Appendix 1 - How to read /include a microstructure file

MICRESS can read initial microstructure and composition or temperature fields from a file. The file to be read should be an ASCII file with a known "geometry" (number of cells in X and Y direction): the dimension of the read- in data set does not need to be identical to the simulation one. The most complex case is probably reading an experimental grain structure, but this is not as daunting as it could seem.

Here is a step-by-step description how to do that using GIMP (GNU Image Manipulation Program), Version 1.2.5 (www.gimp.org). The micrograph is courtesy of IEHK, RWTH Aachen. Newer GIMP versions have similar functionalities but the naming might differ. However, any full-fledged image manipulation program should support similar procedures.

-Image/Transform/Zealous Crop/ to get rid of any frame
-Layers/Layers, Channels & Paths/Layers/: insert a new (transparent) layer
-Select a clearly different "foreground colour"
-Tools/Paint → Tools/Pencil to draw the boundaries on the transparent layer.1.
-Tools/Paint → Tools/Pencil to draw the boundaries on the transparent layer
-Layers/Layers, Channels & Paths/Layers/: remove the "background" layer. Make sure you do not leave any "dangling" boundaries, so that each grain is "closed" (the boundaries of the domain themselves do not have to be re-drawn, as MICRESS will perform this task).
-Image/Mode/Indexed: Use Black/White (1-Bit) Palette
-File/Save as/ save to ".pgm", by "exporting" first. Make sure you save the file in ASCII-code.

Appendix 2 - Input file

```
# Automatic 'Driving File' written out by MICRESS.
#
# MICRESS binary
# ===============
# version number: 6.001 (Windows)
# compiled: 11/15/2011
# compiler version: Intel 1200 20110427
# ('double precision' binary)
# license expires in 87 days
#
# Language settings
# ==================
#  Please select a language: 'English', 'Deutsch' or 'Francais'
English
#
# Flags and settings
# ===================
# Geometry
# --------
# Grid size?
# (for 2D calculations: AnzY=1, for 1D calculations: AnzX=1, AnzY=1)
# AnzX:
450
# AnzY:
1
```

```
# AnzZ:
400
# Cell dimension (grid spacing in micrometers):
# (optionally followed by rescaling factor for the output in the form of '3/4')
0.500
#
# Flags
# -----
# Type of coupling?
# Options: phase concentration temperature temp_cyl_coord
#          [stress] [stress_coupled] [flow]
phase
# Type of potential?
# Options: double_obstacle multi_obstacle [fd_correction]
double_obstacle
#
# Phase field data structure
# --------------------------
# Coefficient for initial dimension of field iFace
# [minimum usage] [target usage]
0.1
# Coefficient for initial dimension of field nTupel
# [minimum usage] [target usage]
0.1
#
# Restart options
# ===============
# Restart using old results?
# Options:   new     restart [reset_time]
new
#
# Name of output files
# ====================
# Name of result files?
Results_Grain_Growth_with_pinning_7/Grain_Growth_with_pinning_7
# Overwrite files with the same name?
# Options:   overwrite    write_protected    append
#          [zipped|not_zipped|vtk_zipped|vtk_not_zipped]
#          [unix|windows|non_native]
overwrite
#
# Selection of the outputs
# ========================
# [legacy|verbose|terse]
#
# Restart data output?                    ('rest')
# Options:   out_restart    no_out_restart      [wallclock time, h.]
no_out_restart
# Grain number output?                    ('korn')
# Options:   out_grains     no_out_grains
out_grains
# Phase number output?                    ('phas')
# Options:   out_phases     no_out_phases       [no_interfaces]
out_phases
```

```
# Fraction output?                          ('frac')
# Options:    out_fraction    no_out_fraction       [phase number]
no_out_fraction
# Average fraction table?                   ('TabF')
# Options:    tab_fractions   no_tab_fractions      [front_temperature]
no_tab_fractions
# Interface output?                         ('intf')
# Options:    out_interface   no_out_interface      [sharp]
out_interface
# Driving-force output?                     ('driv')
# Options:    out_driv_force  no_out_driv_force
out_driv_force
# Interface mobility output?                ('mueS')
# Options:    out_mobility    no_out_mobility
out_mobility
# Curvature output?                         ('krum')
# Options:    out_curvature   no_out_curvature
out_curvature
# Interface velocity output?                ('vel')
# Options:    out_velocity    no_out_velocity
out_velocity
# Should the grain-time file be written out?        ('TabK')
# Options:    tab_grains      no_tab_grains         [extra|standard]
tab_grains
# Should the 'von Neumann Mullins' output be written out?     ('TabN')
# Options:   tab_vnm   no_tab_vnm
tab_vnm
# Should the 'grain data output' be written out?     ('TabGD')
# Options:   tab_grain_data   no_tab_grain_data
tab_grain_data
# Temperature output?                       ('temp')
# Options:    out_temp        no_out_temp
no_out_temp
# Recrystallisation output?                 ('rex')
# Options:    out_recrystall  no_out_recrystall
out_recrystall
# Recrystallysed fraction output?             ('TabR')
# Options:    tab_recrystall  no_tab_recrystall
tab_recrystall
# Miller-Indices output?                    ('mill')
# Options:    out_miller      no_out_miller
no_out_miller
# Orientation output?                       ('orie')
# Options:    out_orientation  no_out_orientation
out_orientation
# Should the orientation-time file be written out?    ('TabO')
# Options:    tab_orientation  no_tab_orientation
tab_orientation
# Should monitoring outputs be written out?         ('TabL')
# Options:    tab_log [simulation time, s] [wallclock time, min]  no_tab_log
no_tab_log 0.5
#
# Time input data
# ===============
```

```
# Finish input of output times (in seconds) with 'end_of_simulation'
# 'regularly-spaced' outputs can be set with 'linear_step'
# or 'logarithmic_step' and then specifying the increment
# and end value
# ('automatic_outputs' optionally followed by the number
#  of outupts can be used in conjuction with 'linear_from_file')
linear_step 0.1 5
linear_step 1 20
linear_step 5 100
linear_step 10 270
end_of_simulation
# Time-step?
# Options: (real)  automatic [0<factor_1<=1] [0<=factor_2] [max.] [min.]
# (Fix time steps: just input the value)
automatic
# Coefficient for phase-field criterion 1.00
# Number of iterations for initialisation?
5
#
# Phase data
# ==========
# Number of distinct solid phases?
1
#
# Data for phase 1:
# ----------------
# Simulation of recrystallisation in phase 1?
# Options:  recrystall  no_recrystall
recrystall
# Is phase 1 anisotrop?
# Options:  isotropic  anisotropic  faceted  antifaceted
anisotropic
# Crystal symmetry of the phase?
# Options:  none  xyz_axis  cubic  hexagonal
cubic
# Should grains of phase 1 be reduced to categories?
# Options:  categorize no_categorize
no_categorize
#
# Orientation
# -----------
# How shall grain orientations be defined?
# Options:  angle_2d
#           euler_zxz
#           angle_axis
#           miller_indices
angle_2d
#
# Grain input
# ===========
# Type of grain positioning?
# Options: deterministic  random  from_file
from_file
# File for grain properties
```

```
Microstructure_400_320.txt
# Treatment of data?
# (n: none, 1: 1D, f: flip (bottom<->top), t: transpose,
#  or p: 'phase to grains transformation')
fp
# AnzX for initial microstructure?
400
# AnzZ for initial microstructure?
320
# Number of grains at the beginning?
# (Set to less than 1 to read from input data,
#  with optionally a minimal size, in cells)
-1
# Read grain properties from a file?
# Options:  input  from_file  identical  blocks
identical
# Input data for grain number 1:
# Phase number?  (integer)
1
# Recrystallisation energy?
3.0000
# Rotation angle? [Degree]
+25.0000
# 'Non-geometric' data for grains 1 to 108 identical
#=====================================================
# Data for further nucleation
# ===========================
# Enable further nucleation?
# Options:  nucleation  no_nucleation  [verbose|no_verbose]
nucleation
# Additional output for nucleation?
# Options:  out_nucleation  no_out_nucleation
no_out_nucleation
#
# Number of types of seeds?
2
#
# Input for seed type 1:
# ----------------------
# Type of 'position' of the seeds?
# Options: bulk region interface triple quadruple [restrictive]
interface
# Phase of new grains?
1
# Reference phase?
1
# Substrat phase [2nd phase in interface]?
# (set to 1 to disable the effect of substrate curvature)
1
# maximum number of new nuclei 1?
50
# Grain radius [micrometers]?
0.61000
# Choice of growth mode:
```

```
# Options:   stabilisation analytical_curvature
stabilisation
# critical recrystallisation energy [J/cm**3]?
2.8000
# Determination of nuclei orientations?
# Options: random fix range parent_relation
random
# Shield effect:
# Shield time [s] ?
180.00
# Shield distance [micrometers]?
1.7
# Input of minimal and maximal recrystallisation energy:
# (dG contribution only if energy is 0 on one side!)
# Minimum of recrystallisation energy? [J/cm**3]
0.0000
# Maximum of recrystallisation energy? [J/cm**3]
0.0000
# Nucleation range
# min. nucleation temperature for seed type 1 [K]
630.0000
# max. nucleation temperature for seed type 1 [K]
700.000
# Time between checks for nucleation? [s]
2.00000E-02
# Shall random noise be applied?
# Options:   nucleation_noise  no_nucleation_noise
no_nucleation_noise
#
# Input for seed type 2:
# ----------------------
# Type of 'position' of the seeds?
# Options: bulk region interface triple quadruple [restrictive]
triple
# Phase of new grains?
1
# Reference phase?
1
# Substrat phase [2nd phase in interface]?
# (set to 1 to disable the effect of substrate curvature)
1
# maximum number of new nuclei 2?
75
# Grain radius [micrometers]?
0.910000
# Choice of growth mode:
# Options:   stabilisation analytical_curvature
stabilisation
# critical recrystallisation energy [J/cm**3]?
2.5000
# Determination of nuclei orientations?
# Options: random fix range parent_relation
random
# Shield effect:
```

```
# Shield time [s] ?
250.0
# Shield distance [micrometers]?
2.00
# Input of minimal and maximal recrystallisation energy:
# (dG contribution only if energy is 0 on one side!)
# Minimum of recrystallisation energy?  [J/cm**3]
0.0000
# Maximum of recrystallisation energy?  [J/cm**3]
0.0000
# Nucleation range
# min. nucleation temperature for seed type 2 [K]
600.0000
# max. nucleation temperature for seed type 2 [K]
750.000
# Time between checks for nucleation? [s]
2.00000E-02
# Shall random noise be applied?
# Options:    nucleation_noise   no_nucleation_noise
no_nucleation_noise
#
# Max. number of simultaneous nucleations?
# ----------------------------------------
# (set to 0 for automatic)
5
#
# Shall metastable small seeds be killed?
# ---------------------------------------
# Options:    kill_metastable     no_kill_metastable
kill_metastable
#
# Phase interaction data
# ======================
# Data for phase interaction 0 / 1:
# ---------------------------------
# Simulation of interaction between phase 0 and 1?
# Options:   phase_interaction    no_phase_interaction
#   [standard|particle_pinning[_temperature]|solute_drag|redistribution_control]
no_phase_interaction
#
# Data for phase interaction 1 / 1:
# ---------------------------------
# Simulation of interaction between phase 1 and 1?
# Options:   phase_interaction    no_phase_interaction
#   [standard|particle_pinning[_temperature]|solute_drag|redistribution_control]
phase_interaction particle_pinning
# Type of surface energy definition between phases 1 and 1?
# Options:  constant  temp_dependent
constant
# Surface energy between phases 1 and 1? [J/cm**2]
1.08000E-04
# Type of mobility definition between phases 1 and 1?
# Options:  constant  temp_dependent  dg_dependent
constant
```

```
# Kinetic coefficient mu between phases 1 and 1? [cm**4/(Js)]
3.800000E-05
# critical pinning force [1/micrometer]
0.9
# minimal mobility [cm**4/Js]
0.0
# Shall misorientation be considered?
# Optionen:   misorientation   no_misorientation
misorientation
# Input of the misorientation coefficient:
# Modification of surface energy for low angle
# boundaries
# (multiplying factor to value for high angle boundaries)
1.0000
# Modification of mobility for low angle
# boundaries
# (multiplying factor to value for high angle boundaries)
1.00000
#
# Boundary conditions
# ===================
# Type of temperature trend?
# Options:  linear    linear_from_file    profiles_from_file
linear
# Number of connecting points?   (integer)
0
# Initial temperature at the bottom?  (real)  [K]
723.15
# Temperature gradient in z-direction?  [K/cm]
0.E+0
# Cooling rate? [K/s]
0.0000
#
# Options:    moving_frame     no_moving_frame
no_moving_frame
# Boundary conditions for phase field in each direction
# Options: i (insulation) s (symmetric) p (periodic/wrap-around)
#          g (gradient)  f (fixed)    w (wetting)
# Sequence: E W (N S, if 3D) B T borders
iiii
#
# Unit-cell model symmetric with respect to the x/y diagonal plane?
# Options:   unit_cell_symm   no_unit_cell_symm
no_unit_cell_symm
#
# Other numerical parameters
# ==========================
# Phase minimum?
1E-04
# Interface thickness (in cells)?
5.00
#
```